

FINITE ELEMENT ANALYSIS FOR THE NAVIER-LAMÉ EIGENVALUE PROBLEM*

FELIPE LEPE[†], GONZALO RIVERA[‡], AND JESUS VELLOJIN[§]

Abstract. The present paper introduces the analysis of the eigenvalue problem for the elasticity equations when the so called Navier-Lamé system is considered. Such a system introduces the displacement, rotation and pressure of some linear and elastic structure. The analysis of the spectral problem is based in the compact operators theory. A finite element method based in polynomials of degree $k \geq 1$ are considered in order to approximate the eigenfrequencies and eigenfunctions of the system. Convergence and error estimate are presented. An a posteriori error analysis is performed, where the reliability and efficiency of the proposed estimator is proved. We end this contribution reporting a series of numerical tests in order to assess the performance of the proposed numerical method, for the a priori and a posteriori estimates.

Key words. Elasticity equations, eigenvalue problems, error estimates, mixed problems

AMS subject classifications. 35Q35, 65N15, 65N25, 65N30, 65N50

1. Introduction. Different approaches to analyze the elasticity equations have been analyzed in the past years, since the stability of different structures plays an important role for the design and construction of more complex structures. The displacement of elastic structures, when external forces are applied, reveals the importance of how structures manifest their behaviors depending on their physical features, which are given by the Lamé constants.

To handle the linear elasticity equations, several formulations and numerical methods have emerged in the past years. In this sense, mixed formulations are a path to avoid the locking phenomenon in the computational implementation that arises when the Lamé constant $\lambda \rightarrow \infty$, leading to the so called nearly incompressible elasticity equations.

In the literature, an important number of contributions related to mixed formulations for elasticity are available such as [3, 4, 7, 12, 15, 14], just to mention some of them. These references have the particularity that the results are focused in the load problems. These contributions are relevant for our work in spectral problems, since in this context, the analysis of load problems provide a source of techniques that can be extended for the eigenvalue approach.

The research related to mixed formulations for the elasticity spectral problem is an ongoing subject and different formulations and methods have emerged, as [8, 19, 21, 1, 24], where these formulations and numerical methods are not only interested in the approximation of the displacement of the structure, but also on other quantities as the pseudostress, the Cauchy stress tensor, the rotations, etc. Moreover, since these

*Submitted to the editors DATE.

Funding: The first author was partially supported by DIUBB through project 2120173 GI/C Universidad del Bío-Bío and ANID-Chile through FONDECYT project 11200529 (Chile). The second author was supported by Universidad de Los Lagos Regular R02/21. The third author was partially supported by ANID-Chile through project Anillo of Computational Mathematics for Desalination Processes ACT210087.

[†]GIMNAP-Departamento de Matemática, Universidad del Bío - Bío, Casilla 5-C, Concepción, Chile. flepe@ubiobio.cl.

[‡]Departamento de Ciencias Exactas, Universidad de Los Lagos, Casilla 933, Osorno, Chile. gonzalo.rivera@ulagos.cl.

[§]GIMNAP-Departamento de Matemática, Universidad del Bío - Bío, Casilla 5-C, Concepción, Chile. jvellojin@ubiobio.cl.

formulations are mixed, the locking phenomenon is avoided and the spectrum of the solution operators is approximated safely with any numerical method.

In the present work, we continue with the analysis of mixed formulations for the elasticity equations and the associated eigenvalue problem, where the formulation analyzed in [3, 4] is considered. These works concern the Navier-Lamé formulation of the elasticity equations, where not only the displacement of the structure is the unknown, but also the vorticity and pressure of the structure. The proposed mixed formulation, compared with the one analyzed in [19], avoids the $H(\text{div})$ spaces and allows to handle more simple Hilbert spaces as L^2 and H^1 . The advantage behind this approach is the relaxation of the finite element spaces where the solutions are approximated by means of continuous polynomials for the displacement and discontinuous elements for the pressure and vorticity. The above establishes a difference with respect to the use of Raviart-Thomas or Brezzi-Douglas-Marini elements, classic in the $H(\text{div})$ approach.

With this Navier-Lamé eigensystem, our goal is to analyze a mixed finite element method for which we obtain a priori and a posteriori error estimates. These two analysis are important since the a priori analysis not only gives us the basic convergence results and error estimates, but also the spurious free feature of the method, whereas the a posteriori analysis takes relevance when the eigenfunctions of the spectral problem are not smooth enough when the geometries of certain domains or physical parameters are not sufficiently suitable to recover the optimal order of convergence given by the a priori analysis. The a priori analysis is based on the classic theory of compact operators given by [6], where the convergence of eigenvalues and eigenfunctions is obtained with standard arguments. Also, we derive an error estimate for the displacement of the structure in the L^2 norm, with a duality argument. Controlling this error is important since it arises naturally when performing the analysis of the reliability and efficiency of the a posteriori estimator.

The paper is organized in the following way: In Section 2 we present the model problem, where we introduce the classic elasticity eigenvalue problem and, with some algebraic manipulations, we write the Navier-Lamé system of our interest. We define the bilinear forms that we need for the analysis and recall a well posedness result, fundamental to introduce the solution operator that will be involved along the manuscript. A spectral characterization of this operator is presented. In Section 3 we introduce the tools for the numerical analysis, namely, definitions and properties associated to the meshes, the finite element spaces, the discrete eigenvalue problem, and the discrete solution operator. This allows us to conclude a convergence result. This section contains the core of our paper, since the a priori and a posteriori analysis are reported, where we prove basic error estimates for the eigenvalues and eigenfunctions, together with the analysis of an a posteriori error estimator, whose reliability and efficiency is proven. Finally, in Section 4, we present a series of numerical tests in order to confirm the theoretical results that we present. These results, that we perform in two and three dimensions, show that the a priori error estimates are attained at computational level, and that the a posteriori error estimator that we propose is capable to perform an adaptive refinement in order to recover the optimal order of convergence, for nonregular eigenfunctions.

2. The model problem. Let $\Omega \subset \mathbb{R}^n$, with $n \in \{2, 3\}$, be an open bounded domain with Lipschitz boundary $\partial\Omega$. To derive the problem of our interest, we need

to recall the elasticity eigenvalue problem given as follows

$$(2.1) \quad \begin{cases} \operatorname{div}(2\mu_s \boldsymbol{\varepsilon}(\mathbf{u}) + \lambda_s \operatorname{div} \mathbf{u} \mathbf{I}) &= -\kappa \mathbf{u} & \text{in } \Omega, \\ \mathbf{u} &= \mathbf{0} & \text{on } \partial\Omega, \end{cases}$$

where \mathbf{u} is the displacement, $\mathbf{I} \in \mathbb{R}^{n \times n}$ is the identity tensor, λ_s and μ_s are de Lamé constants and $\boldsymbol{\varepsilon}(\cdot)$ is the strain tensor given by $\boldsymbol{\varepsilon}(\mathbf{u}) := \frac{1}{2}(\nabla \mathbf{u} + (\nabla \mathbf{u})^\top)$. For the derivation of the Navier-Lamé system, as a first ingredient, we need the following identity

$$\operatorname{div}(\boldsymbol{\varepsilon}(\mathbf{u})) = \frac{1}{2}(\Delta \mathbf{u} + \nabla(\operatorname{div} \mathbf{u})).$$

With this identity at hand, and replacing it in (2.1), we arrive to the following system

$$\begin{cases} \mu_s \Delta \mathbf{u} + (\mu_s + \lambda_s) \nabla(\operatorname{div} \mathbf{u}) &= -\kappa \mathbf{u} & \text{in } \Omega, \\ \mathbf{u} &= \mathbf{0} & \text{on } \partial\Omega. \end{cases}$$

Now, defining the pressure p by $p := -(2\mu_s + \lambda_s) \operatorname{div} \mathbf{u}$, we obtain the following displacement-pressure system

$$\begin{cases} \mu_s \Delta \mathbf{u} - \nabla p &= -\kappa \mathbf{u} & \text{in } \Omega, \\ \operatorname{div} \mathbf{u} + (2\mu_s + \lambda_s)^{-1} p &= 0 & \text{in } \Omega, \\ \mathbf{u} &= \mathbf{0} & \text{on } \partial\Omega. \end{cases}$$

Introducing the field of scaled rotations by $\boldsymbol{\omega} := \sqrt{\mu_s} \operatorname{curl} \mathbf{u}$, we obtain the following rotation-pressure-displacement system

$$(2.2) \quad \begin{cases} \sqrt{\mu_s} \operatorname{curl} \boldsymbol{\omega} + \nabla p &= \kappa \mathbf{u} & \text{in } \Omega, \\ \boldsymbol{\omega} - \sqrt{\mu_s} \operatorname{curl} \mathbf{u} &= 0 & \text{in } \Omega, \\ \operatorname{div} \mathbf{u} + (2\mu_s + \lambda_s)^{-1} p &= 0 & \text{in } \Omega, \\ \mathbf{u} &= \mathbf{0} & \text{on } \partial\Omega. \end{cases}$$

Now we introduce a variational formulation for (2.2). To do this task, we multiply such a system with suitable test functions, integrate by parts, and use the boundary conditions in order to obtain the following bilinear forms $a : L^2(\Omega)^{n(n-1)/2} \times L^2(\Omega) \rightarrow \mathbb{R}$ and $b : (L^2(\Omega)^{n(n-1)/2} \times L^2(\Omega)) \times H^1(\Omega)^n \rightarrow \mathbb{R}$ defined by

$$a((\boldsymbol{\omega}, p), (\boldsymbol{\theta}, q)) := \int_{\Omega} \boldsymbol{\omega} \cdot \boldsymbol{\theta} + (2\mu_s + \lambda_s)^{-1} \int_{\Omega} pq,$$

and

$$b((\boldsymbol{\theta}, q), \mathbf{u}) := \int_{\Omega} \operatorname{div} \mathbf{u} q - \sqrt{\mu_s} \int_{\Omega} \boldsymbol{\theta} \cdot \operatorname{curl} \mathbf{u}.$$

With these bilinear forms at hand, we write the following weak formulation for problem (2.2): Find $\lambda \in \mathbb{R}$ and $((\boldsymbol{\omega}, p), \mathbf{u}) \in L^2(\Omega)^{n(n-1)/2} \times L^2(\Omega) \times H^1(\Omega)^n$ such that

$$(2.3) \quad \begin{cases} a((\boldsymbol{\omega}, p), (\boldsymbol{\theta}, q)) + b((\boldsymbol{\theta}, q), \mathbf{u}) &= 0 & \forall (\boldsymbol{\theta}, q) \in L^2(\Omega)^{n(n-1)/2} \times L^2(\Omega), \\ b((\boldsymbol{\omega}, p), \mathbf{v}) &= \kappa(\mathbf{u}, \mathbf{v}) & \forall \mathbf{v} \in H^1(\Omega)^n. \end{cases}$$

Now we define the following bilinear form

$$\mathcal{A}((\mathbf{u}, \boldsymbol{\omega}, p), (\mathbf{v}, \boldsymbol{\theta}, q)) := a((\boldsymbol{\omega}, p), (\boldsymbol{\theta}, q)) + b((\boldsymbol{\theta}, q), \mathbf{u}) + b((\boldsymbol{\omega}, p), \mathbf{v}).$$

With this definition at hand, the weak eigenvalue problem associated to (2.3) is stated below.

PROBLEM 2.1. Find $\lambda \in \mathbb{R}$ and $\mathbf{0} \neq (\mathbf{u}, \boldsymbol{\omega}, p) \in \mathbf{H}_0^1(\Omega)^n \times \mathbf{L}^2(\Omega)^{n(n-1)/2} \times \mathbf{L}^2(\Omega)$, such that

$$(2.4) \quad \mathcal{A}((\mathbf{u}, \boldsymbol{\omega}, p), (\mathbf{v}, \boldsymbol{\theta}, q)) = -\kappa(\mathbf{u}, \mathbf{v})_{0,\Omega},$$

for all $(\mathbf{v}, \boldsymbol{\theta}, q) \in \mathbf{H}_0^1(\Omega)^n \times \mathbf{L}^2(\Omega)^{n(n-1)/2} \times \mathbf{L}^2(\Omega)$.

Since we have a prescribed Dirichlet condition on $\partial\Omega$, then the pressure needs to satisfy the zero-mean condition in order to control the norm in $\mathbf{L}^2(\Omega)$ as we approach to the incompressible limit $\nu = 0.5$. Following [4], the pressure is decomposed by $p = p_0 + P_m p$, where $P_m p$ and p_0 are the mean value and zero-mean value parts of the pressure, and obtain the following result [4, Theorem 2.1].

LEMMA 2.2. For all $\mathbf{0} \neq (\mathbf{u}, \boldsymbol{\omega}, p) \in \mathbf{H}_0^1(\Omega)^n \times \mathbf{L}^2(\Omega)^{n(n-1)/2} \times \mathbf{L}^2(\Omega)$, there exists $(\mathbf{v}, \boldsymbol{\theta}, q) \in \mathbf{H}_0^1(\Omega)^n \times \mathbf{L}^2(\Omega)^{n(n-1)/2} \times \mathbf{L}^2(\Omega)$ with $\|(\mathbf{v}, \boldsymbol{\theta}, q)\| \leq C \|(\mathbf{u}, \boldsymbol{\omega}, p)\|$ such that

$$\mathcal{A}((\mathbf{u}, \boldsymbol{\omega}, p), (\mathbf{v}, \boldsymbol{\theta}, q)) \geq C \|(\mathbf{u}, \boldsymbol{\omega}, p)\|^2,$$

where the triple norm is defined by

$$\begin{aligned} \|(\mathbf{v}, \boldsymbol{\theta}, q)\|^2 := & \mu_s \|\mathbf{curl} \mathbf{v}\|_{0,\Omega}^2 + \mu_s \|\operatorname{div} \mathbf{v}\|_{0,\Omega}^2 + \|\boldsymbol{\theta}\|_{0,\Omega}^2 \\ & + (2\mu_s + \lambda_s)^{-1} \|q\|_{0,\Omega}^2 + \mu_s^{-1} \|q_0\|_{0,\Omega}^2. \end{aligned}$$

Let us define the solution operator associated to the eigenvalue problem. Let \mathbf{T} be such an operator, which is linear and defined by

$$\mathbf{T} : \mathbf{H}_0^1(\Omega)^n \rightarrow \mathbf{H}_0^1(\Omega)^n, \quad \mathbf{f} \mapsto \mathbf{T}\mathbf{f} := \tilde{\mathbf{u}},$$

where the triplet $(\tilde{\mathbf{u}}, \tilde{\boldsymbol{\omega}}, \tilde{p})$ is the solution of the following well posed source problem

$$(2.5) \quad \mathcal{A}((\tilde{\mathbf{u}}, \tilde{\boldsymbol{\omega}}, \tilde{p}), (\mathbf{v}, \boldsymbol{\theta}, q)) = -(\mathbf{f}, \mathbf{v})_{0,\Omega},$$

for all $(\mathbf{v}, \boldsymbol{\theta}, q) \in \mathbf{H}_0^1(\Omega)^n \times \mathbf{L}^2(\Omega)^{n(n-1)/2} \times \mathbf{L}^2(\Omega)$. As a consequence of Lemma 2.2, an application of the Babüska-Brezzi theory reveals that the operator \mathbf{T} is well defined and bounded. Observe that \mathbf{T} is selfadjoint with respect to the $\mathbf{L}^2(\Omega)$ inner product. Indeed, let \mathbf{f} and $\tilde{\mathbf{f}}$ be such that $\mathbf{u} = \mathbf{T}\mathbf{f}$ and $\tilde{\mathbf{u}} = \mathbf{T}\tilde{\mathbf{f}}$. Then, from the symmetry of $a(\cdot, \cdot)$ we have

$$\begin{aligned} (\mathbf{f}, \mathbf{T}\tilde{\mathbf{f}})_{0,\Omega} &= (\mathbf{f}, \tilde{\mathbf{u}})_{0,\Omega} = b((\boldsymbol{\omega}, p), \tilde{\mathbf{u}}) = -a((\tilde{\boldsymbol{\omega}}, \tilde{p}), (\boldsymbol{\omega}, p)) \\ &= -a((\boldsymbol{\omega}, p), (\tilde{\boldsymbol{\omega}}, \tilde{p})) = b((\tilde{\boldsymbol{\omega}}, \tilde{p}), \mathbf{u}) = (\tilde{\mathbf{f}}, \mathbf{u})_{0,\Omega} = (\tilde{\mathbf{f}}, \mathbf{T}\mathbf{f})_{0,\Omega} = (\mathbf{T}\mathbf{f}, \tilde{\mathbf{f}})_{0,\Omega}. \end{aligned}$$

Let η be a real number such that $\eta \neq 0$. Notice that $(\eta, \mathbf{u}) \in \mathbb{R} \times \mathbf{H}_0^1(\Omega)^n$ is an eigenpair of \mathbf{T} if and only if there exists $(\boldsymbol{\omega}, p) \in \mathbf{L}^2(\Omega)^{n(n-1)/2} \times \mathbf{L}^2(\Omega)$ such that, $(\kappa, \mathbf{u}, \boldsymbol{\omega}, p)$ solves Problem 2.1 with $\eta := 1/\kappa$.

A key ingredient for the numerical analysis of Problem 2.1 is the following regularity result for the source problem, which is a direct consequence of Lemma 2.2 (see [3, Theorem 2.1]) and the well-known regularity for the elasticity equations (see, for instance, [17] and [25, Theorem 5.2]).

THEOREM 2.3 (Regularity). System (2.5) has a unique solution and there exists a positive constant C such that

$$\|(\tilde{\mathbf{u}}, \tilde{\boldsymbol{\omega}}, \tilde{p})\| \leq C \|\mathbf{f}\|_{0,\Omega}.$$

Moreover, there exists $\widehat{s} \in (0, 1]$ such that for all $s \in (0, \widehat{s})$, we have $\widetilde{\mathbf{u}} \in \mathbf{H}^{1+s}(\Omega)^n$ and

$$\|\widetilde{\mathbf{u}}\|_{1+s,\Omega} + \|\widetilde{\boldsymbol{\omega}}\|_{s,\Omega} + \|\widetilde{p}\|_{s,\Omega} \leq \widehat{C}\|\mathbf{f}\|_{0,\Omega},$$

where $\widehat{C} > 0$ which in principle depends on λ_s . On the other hand, the regularity for the eigenfunctions is as follows

$$\|\mathbf{u}\|_{1+s,\Omega} + \|\boldsymbol{\omega}\|_{s,\Omega} + \|p\|_{s,\Omega} \leq \widehat{C}\|\mathbf{u}\|_{0,\Omega}.$$

Hence, \mathbf{T} is a compact operator thanks to the compact inclusion of $\mathbf{H}^{1+s}(\Omega)^n$ onto $\mathbf{H}^1(\Omega)^n$. Now we are in position to present the following spectral characterization for \mathbf{T} .

THEOREM 2.4 (Spectral characterization). *The spectrum of the operator \mathbf{T} decomposes by $\text{sp}(\mathbf{T}) := \{\mu_k\}_{k \in \mathbb{N}} \cup \{0\}$, where $\{\mu_k\}_{k \in \mathbb{N}}$ is a sequence of positive eigenvalues converging to zero. These eigenvalues are repeated according to their respective multiplicities.*

3. Finite element discretization. The aim of this section is to develop a numerical method to approximate the eigenfrequencies of Problem 2.1. We state several results in order to provide estimates that allow to control the corresponding eigenfunctions.

3.1. Mesh properties. Let $\{\mathcal{T}_h\}_{h>0}$ be a shape-regular family of partitions of Ω that, depending on the domain, will consist in triangles (for two dimensions) or tetrahedrons (in three dimensions). Let h_T be the diameter of a triangle $T \in \mathcal{T}_h$ and let us define $h := \max\{h_T : T \in \mathcal{T}_h\}$.

For $T \in \mathcal{T}_h$, let $\mathcal{E}(T)$ be the set of its edges/faces, and let \mathcal{E}_h be the set of all the faces/edges of the triangulation \mathcal{T}_h . For this set, we denote by h_e the corresponding diameter of a face/edge e . With these definitions at hand, we write $\mathcal{E}_h = \mathcal{E}_h(\Omega) \cup \mathcal{E}_h(\partial\Omega)$, where

$$\mathcal{E}_h(\Omega) := \{e \in \mathcal{E}_h : e \subseteq \Omega\} \quad \text{and} \quad \mathcal{E}_h(\partial\Omega) := \{e \in \mathcal{E}_h : e \subseteq \partial\Omega\}.$$

Additionally, we will denote by $\llbracket \cdot \rrbracket$ the corresponding edge/face jump for scalars and vector functions.

Let us introduce the finite element spaces which we will operate. Given $k \geq 1$, the finite element spaces to develop the numerical scheme are the following

$$\begin{aligned} \mathbf{H}_h &:= \{\mathbf{v}_h \in \mathbf{H}_0^1(\Omega) : \mathbf{v}_h|_T \in \mathbb{P}_k(T)^n \quad \forall T \in \mathcal{T}_h\}, \\ \mathbf{Z}_h &:= \{\boldsymbol{\theta}_h \in \mathbf{L}^2(\Omega)^{n(n-1)/2} : \boldsymbol{\theta}_h|_T \in \mathbb{P}_{k-1}(T)^{n(n-1)/2} \quad \forall T \in \mathcal{T}_h\}, \\ Q_h &:= \{q_h \in \mathbf{L}^2(\Omega) : q_h|_T \in \mathbb{P}_{k-1}(T) \quad \forall T \in \mathcal{T}_h\}, \end{aligned}$$

in which the rotation, displacement, and pressure are approximated, respectively.

3.2. Discrete problem. We start this section by stating the corresponding finite element discretization of Problem 2.1, which reads as follows.

PROBLEM 3.1. *Find $\kappa_h \in \mathbb{R}$ and $\mathbf{0} \neq (\mathbf{u}_h, \boldsymbol{\omega}_h, p_h) \in \mathbf{H}_h \times \mathbf{Z}_h \times Q_h$, such that*

$$\mathcal{A}((\mathbf{u}_h, \boldsymbol{\omega}_h, p_h), (\mathbf{v}_h, \boldsymbol{\theta}_h, q_h)) = -\kappa_h(\mathbf{u}_h, \mathbf{v}_h)_{0,\Omega},$$

for all $(\mathbf{v}_h, \boldsymbol{\theta}_h, q_h) \in \mathbf{H}_h \times \mathbf{Z}_h \times Q_h$.

At this point we must emphasize what was commented in [4, Section 2.2], where we have that the fact that the non-uniqueness of the pressure in the incompressible limit requires that Lagrange multipliers be introduced to fix the zero-mean condition, or, as was done in [18], to add a stabilization term in the case that the pressure is approximated using discontinuous elements (see Section 4 below).

By means of the arguments used in Theorem, we conclude that Problem 3.1 is well-posed, and therefore we have the respective discrete estimates for the discrete source problem.

Let \mathbf{T}_h be the discrete linear operator defined by

$$\mathbf{T}_h : H^{1+s}(\Omega)^n \rightarrow \mathbf{H}_h, \quad \mathbf{f} \mapsto \mathbf{T}_h \mathbf{f} := \tilde{\mathbf{u}}_h,$$

where the triplet $(\tilde{\mathbf{u}}_h, \tilde{\boldsymbol{\omega}}_h, \tilde{p}_h)$ is the solution of the following discrete source problem

$$(3.1) \quad \mathcal{A}((\tilde{\mathbf{u}}_h, \tilde{\boldsymbol{\omega}}_h, \tilde{p}_h), (\mathbf{v}_h, \boldsymbol{\theta}_h, q_h)) = -(\mathbf{f}, \mathbf{v}_h)_{0,\Omega},$$

for all $(\mathbf{v}_h, \boldsymbol{\theta}_h, q_h) \in \mathbf{H}_h \times \mathbf{Z}_h \times Q_h$. Observe that \mathbf{T}_h is selfadjoint and as in the continuous case, $(\eta_h, \mathbf{u}_h) \in \mathbb{R} \times \mathbf{H}_h$, with $\eta_h \neq 0$, is an eigenpair of \mathbf{T}_h if only if there exists $(\boldsymbol{\omega}_h, p_h) \in \mathbf{Z}_h \times Q_h$ such that, $(\kappa_h, \mathbf{u}_h, \boldsymbol{\omega}_h, p_h)$ solves Problem 3.1 for $\eta_h := 1/\kappa_h$.

The following result is a direct consequence of the well-posedness of Problems 2.1–3.1 and their corresponding source problems.

COROLLARY 3.2 (Approximation between \mathbf{T} and \mathbf{T}_h). *Let $\mathbf{f} \in L^2(\Omega)^n$. Under the assumptions of Theorem 2.3, there exists $C_{\mu_s} > 0$, independent of h , such that*

$$\|(\mathbf{T} - \mathbf{T}_h)\mathbf{f}\|_{1,\Omega} \leq C_{\mu_s} h^s \|\mathbf{f}\|_{0,\Omega} \leq C_{\mu_s} h^s \|\mathbf{f}\|_{1,\Omega}.$$

Proof. Let $\tilde{\mathbf{u}} := \mathbf{T}\mathbf{f}$ and $\tilde{\mathbf{u}}_h := \mathbf{T}_h\mathbf{f}$. Hence, we have directly

$$\|(\mathbf{T} - \mathbf{T}_h)\mathbf{f}\|_{1,\Omega} = \|\tilde{\mathbf{u}} - \tilde{\mathbf{u}}_h\|_{1,\Omega} \leq \frac{1}{\sqrt{\mu_s}} \|\|(\tilde{\mathbf{u}} - \tilde{\mathbf{u}}_h, \tilde{\boldsymbol{\omega}} - \tilde{\boldsymbol{\omega}}_h, \tilde{p} - \tilde{p}_h)\|\|.$$

From [3, Theorem 3.1], the following best approximation property holds

$$\|\|(\tilde{\boldsymbol{\omega}} - \tilde{\boldsymbol{\omega}}_h, \tilde{p} - \tilde{p}_h, \tilde{\mathbf{u}} - \tilde{\mathbf{u}}_h)\|\| \leq C \inf_{(\mathbf{v}_h, \boldsymbol{\theta}_h, q_h) \in \mathbf{H}_h \times \mathbf{Z}_h \times Q_h} \|\|(\tilde{\boldsymbol{\omega}} - \boldsymbol{\theta}_h, \tilde{p} - q_h, \tilde{\mathbf{u}} - \mathbf{v}_h)\|\|,$$

where the constant C is positive and independent of h . The result is concluded from [3, Theorem 3.2] and the additional regularity provided by Theorem 2.3. \square

Remark 3.3. We note from the above corollary that the following result is also true

$$(3.2) \quad \|\|(\tilde{\mathbf{u}} - \tilde{\mathbf{u}}_h, \tilde{\boldsymbol{\omega}} - \tilde{\boldsymbol{\omega}}_h, \tilde{p} - \tilde{p}_h)\|\| \leq C_{\mu_s} h^s \|\mathbf{f}\|_{1,\Omega}.$$

As a consequence of the previous results, it is immediate that the proposed numerical method is spurious free, as is stated in the following result (see [20] for instance).

THEOREM 3.4. *Let $V \subset \mathbb{C}$ be an open set containing $\text{sp}(\mathbf{T})$. Then, there exists $h_0 > 0$ such that $\text{sp}(\mathbf{T}_h) \subset V$ for all $h < h_0$.*

Let us recall the definition of the resolvent operator of \mathbf{T} and \mathbf{T}_h respectively:

$$\begin{aligned} R_z(\mathbf{T}) &:= (z\mathbf{I} - \mathbf{T})^{-1} : H_0^1(\Omega)^n \rightarrow H_0^1(\Omega)^n, \quad z \in \mathbb{C} \setminus \text{sp}(\mathbf{T}), \\ R_z(\mathbf{T}_h) &:= (z\mathbf{I} - \mathbf{T}_h)^{-1} : \mathbf{H}_h \rightarrow \mathbf{H}_h, \quad z \in \mathbb{C} \setminus \text{sp}(\mathbf{T}_h). \end{aligned}$$

We also invoke the following result for the resolvent of \mathbf{T} .

PROPOSITION 3.5. *If $z \notin \text{sp}(\mathbf{T})$, then there exists a positive constant C , independent of λ and z such that*

$$\|(z\mathbf{I} - \mathbf{T})\mathbf{u}\|_{1,\Omega} \geq C \text{dist}(z, \text{sp}(\mathbf{T}))\|\mathbf{u}\|_{1,\Omega},$$

where $\text{dist}(z, \text{sp}(\mathbf{T}))$ represents the distance between z and the spectrum of \mathbf{T} in the complex plane, which in principle depends on λ_s .

Proof. See [23, Proposition 2.4]. \square

Now we prove the analogous result presented above, but for the resolvent of the discrete solution operator:

LEMMA 3.6. *Let $F \subset \rho(\mathbf{T})$ be closed. Then, there exist positive constants C and h_0 , independent of h , such that for $h < h_0$*

$$\|(z\mathbf{I} - \mathbf{T}_h)^{-1}\mathbf{f}\|_{1,\Omega} \leq C_{\mu_s}\|\mathbf{f}\|_{1,\Omega} \quad \forall z \in F.$$

Our next task is to derive error estimates for the eigenvalues and eigenfunctions. Let $\mathbf{E} : \mathbf{Q} \rightarrow \mathbf{Q}$ be the spectral projector of \mathbf{T} corresponding to the isolated eigenvalue ξ , namely

$$\mathbf{E} := \frac{1}{2\pi i} \int_{\gamma} R_z(\mathbf{T}) dz.$$

On the other, we define $\mathbf{E}_h : \mathbf{Q} \rightarrow \mathbf{Q}$ as the spectral projector of \mathbf{T}_h corresponding to the isolated eigenvalue ξ_h , namely

$$\mathbf{E}_h := \frac{1}{2\pi i} \int_{\gamma} R_z(\mathbf{T}_h) dz.$$

Let κ be an isolated eigenvalue of \mathbf{T} . We define the following distance

$$\mathbf{d}_{\kappa} := \frac{1}{2} \text{dist}(\kappa, \text{sp}(\mathbf{T}) \setminus \{\kappa\}).$$

With this distance at hand, we define the disk centered in κ and boundary γ as follows $D_{\kappa} := \{z \in \mathbb{C} : |z - \kappa| \leq \mathbf{d}_{\kappa}\}$. We observe that the disk defined above satisfies $D_{\kappa} \cap \text{sp}(\mathbf{T}) = \{\kappa\}$.

We owe the following result to [21, Lemma 5.3].

LEMMA 3.7. *Let $\mathbf{f} \in \mathbf{Q}$. There exist constants $C_{\mu_s} > 0$ and $h_0 > 0$ such that, for all $h < h_0$,*

$$\|(\mathbf{E} - \mathbf{E}_h)\mathbf{f}\|_{1,\Omega} \leq \frac{C_{\mu_s}}{\mathbf{d}_{\kappa}} \|(\mathbf{T} - \mathbf{T}_h)\mathbf{f}\|_{1,\Omega} \leq \frac{C_{\mu_s}}{\mathbf{d}_{\kappa}} h^{\min\{s,k\}} \|\mathbf{f}\|_{1,\Omega}.$$

3.3. A priori error estimates. Now our aim is to obtain error estimates for the eigenfunctions and eigenvalues. with our method. We begin by noticing that, according to Corollary 3.2, if $\eta \in (0, 1)$ is an isolated eigenvalue of \mathbf{T} with multiplicity m , and \mathfrak{E} its associated eigenspace, then, there exist m eigenvalues $\eta_h^{(1)}, \dots, \eta_h^{(m)}$ of \mathbf{T}_h , repeated according to their respective multiplicities, which converge to η . Let \mathfrak{E}_h be the direct sum of their corresponding associated eigenspaces (see [20]) and let us define the *gap* $\widehat{\delta}$ between two closed subspaces \mathcal{X} and \mathcal{Y} of $H^1(\Omega)^n$ by

$$\widehat{\delta}(\mathcal{X}, \mathcal{Y}) := \max\{\delta(\mathcal{X}, \mathcal{Y}), \delta(\mathcal{Y}, \mathcal{X})\}, \quad \text{where } \delta(\mathcal{X}, \mathcal{Y}) := \sup_{\substack{x \in \mathcal{X} \\ \|x\|_{1,\Omega}=1}} \left(\inf_{y \in \mathcal{Y}} \|x - y\|_{1,\Omega} \right).$$

With these definitions and hand, we derive the following error estimates for eigenfunctions and eigenvalues. Since the proof is direct from applying the results of [6, 9, 10], we do not incorporate further details.

THEOREM 3.8. *For $k \geq 1$, the following error estimates for the eigenfunctions and eigenvalues hold*

$$\widehat{\delta}(\mathfrak{E}, \mathfrak{E}_h) \leq \frac{C_{\mu_s}}{\mathfrak{d}_\kappa} h^{\min\{s,k\}} \quad \text{and} \quad |\eta - \eta_h(i)| \leq \frac{C_{\mu_s}}{\mathfrak{d}_\kappa} h^{\min\{s,k\}},$$

where the hidden constants are independent of h .

The following result states a preliminary error estimate for the eigenvalues.

LEMMA 3.9. *Let $(\kappa, \mathbf{u}, \boldsymbol{\omega}, p) \in \mathbb{R} \times \mathbf{H}_0^1(\Omega)^n \times \mathbf{L}^2(\Omega)^{n(n-1)/2} \times \mathbf{L}^2(\Omega)$ be the solution of Problem 2.1 with $\|\mathbf{u}\|_{1,\Omega} = 1$ and let $(\kappa_h, \mathbf{u}_h, \boldsymbol{\omega}_h, p_h) \in \mathbb{R} \times \mathbf{H}_h \times \mathbf{Z}_h \times Q_h$ be its finite element approximation given as the solution of Problem 3.1 with $\|\mathbf{u}_h\|_{1,\Omega} = 1$. Then, there exists $C_{\mu_s} > 0$ such that*

$$\|(\mathbf{u} - \mathbf{u}_h, \boldsymbol{\omega} - \boldsymbol{\omega}_h, p - p_h)\| \leq \frac{C_{\mu_s}}{\mathfrak{d}_\kappa} h^{\min\{s,k\}}.$$

Proof. The result follows by adapting the proof of [22, Lemma 12] to our spectral problem. \square

We are now in position to provide an improvement in the order of convergence presented in Theorem 3.8.

THEOREM 3.10. *For $k \geq 1$, there exists a strictly positive constant such that, for $h < h_0$ there holds*

$$|\kappa - \kappa_h| \leq \frac{C_{\mu_s}}{\mathfrak{d}_\kappa^2} h^{2\min\{s,k\}},$$

where $C_{\mu_s} > 0$, is independent of h .

Proof. Let us define $\mathbf{U} := (\mathbf{u}, \boldsymbol{\omega}, p)$ and $\mathbf{U}_h := (\mathbf{u}_h, \boldsymbol{\omega}_h, p_h)$ with $\|\mathbf{u}\|_{1,\Omega} = \|\mathbf{u}_h\|_{1,\Omega} = 1$. Recalling the definition of $\mathcal{A}(\cdot, \cdot)$ given in (2.4) and the previous definitions, we consider the following eigenvalue problems

$$\mathcal{A}(\mathbf{U}, \mathbf{U}) = -\kappa(\mathbf{u}, \mathbf{u}), \quad \mathcal{A}(\mathbf{U}_h, \mathbf{U}_h) = -\kappa_h(\mathbf{u}_h, \mathbf{u}_h),$$

and the well known identity

$$(\kappa - \kappa_h)(\mathbf{u}_h, \mathbf{u}_h) = \mathcal{A}(\mathbf{U} - \mathbf{U}_h, \mathbf{U} - \mathbf{U}_h) + \kappa(\mathbf{u} - \mathbf{u}_h, \mathbf{u} - \mathbf{u}_h)_{0,\Omega}.$$

Taking absolute value to this identity, we obtain that

$$|(\kappa - \kappa_h)(\mathbf{u}_h, \mathbf{u}_h)| \leq \underbrace{|\mathcal{A}(\mathbf{U} - \mathbf{U}_h, \mathbf{U} - \mathbf{U}_h)|}_{\mathbf{I}} + \underbrace{|\kappa(\mathbf{u} - \mathbf{u}_h, \mathbf{u} - \mathbf{u}_h)_{0,\Omega}|}_{\mathbf{II}}.$$

For the term **I**, let us consider the decompositions $p = p_0 + P_m p$ and $p_h = p_{0,h} + P_m p_h$.

Then, using that $\mathbf{u} = \mathbf{u}_h = \mathbf{0}$ on $\partial\Omega$ and integration by parts we have

$$\begin{aligned}
& |\mathcal{A}(\mathbf{U} - \mathbf{U}_h, \mathbf{U} - \mathbf{U}_h)| \\
& \leq |a((\boldsymbol{\omega} - \boldsymbol{\omega}_h, p - p_h), (\boldsymbol{\omega} - \boldsymbol{\omega}_h, p - p_h))| + 2|b((\boldsymbol{\omega} - \boldsymbol{\omega}_h, p - p_h), \mathbf{u} - \mathbf{u}_h)| \\
& \leq \|\boldsymbol{\omega} - \boldsymbol{\omega}_h\|_{0,\Omega}^2 + (2\mu_s + \lambda_s)^{-1} \|p - p_h\|_{0,\Omega}^2 \\
& \quad + 2 \int_{\Omega} |\operatorname{div}(\mathbf{u} - \mathbf{u}_h)(p - p_h)| + 2\sqrt{\mu_s} \int_{\Omega} |(\boldsymbol{\omega} - \boldsymbol{\omega}_h) \cdot \operatorname{curl}(\mathbf{u} - \mathbf{u}_h)| \\
& \leq \mu_s \|\operatorname{curl}(\mathbf{u} - \mathbf{u}_h)\|_{0,\Omega}^2 + 2\|\boldsymbol{\omega} - \boldsymbol{\omega}_h\|_{0,\Omega}^2 + \mu_s^{-1} \|p_0 - p_{0,h}\|_{0,\Omega}^2 \\
& \quad + \mu_s \|\operatorname{div}(\mathbf{u} - \mathbf{u}_h)\|_{0,\Omega}^2 + (2\mu_s + \lambda_s)^{-1} \|p - p_h\|_{0,\Omega}^2 \\
& \leq C \|\!(\mathbf{u} - \mathbf{u}_h, \boldsymbol{\omega} - \boldsymbol{\omega}_h, p - p_h)\!\|^2,
\end{aligned}$$

with $C = 2$. on the other hand, for the term **II** it follows that

$$\begin{aligned}
|\kappa(\mathbf{u} - \mathbf{u}_h, \mathbf{u} - \mathbf{u}_h)_{0,\Omega}| & \leq |\kappa| \|\mathbf{u} - \mathbf{u}_h\|_{0,\Omega}^2 \leq \frac{|\kappa|}{\mu_s} \|\mathbf{u} - \mathbf{u}_h\|_{1,\Omega}^2 \\
& \leq \frac{|\kappa|}{\mu_s} \|\!(\mathbf{u} - \mathbf{u}_h, \boldsymbol{\omega} - \boldsymbol{\omega}_h, p - p_h)\!\|^2.
\end{aligned}$$

Observe that from Lemma 3.9, we have

$$\|\!(\mathbf{u} - \mathbf{u}_h, \boldsymbol{\omega} - \boldsymbol{\omega}_h, p - p_h)\!\|^2 \leq \frac{C_{\mu_s}}{d_{\kappa}^2} h^{2\min\{s,k\}}.$$

On the other hand, by Lemma 2.2 and Poincaré inequality, together with the fact that $\kappa_h^{(i)} \rightarrow \kappa$ as h goes to 0, we have

$$(\mathbf{u}_h, \mathbf{u}_h) = \frac{\mathcal{A}(\mathbf{U}_h, \mathbf{U}_h)}{\kappa_h} \geq C_{\mu_s} \frac{\|\mathbf{u}_h\|_{1,\Omega}^2}{\kappa_h} > 0.$$

This concludes the proof. \square

Remark 3.11. From the above proof it is easy to note that

$$|\kappa - \kappa_h| \leq C_{\mu_s} \|\!(\mathbf{u} - \mathbf{u}_h, \boldsymbol{\omega} - \boldsymbol{\omega}_h, p - p_h)\!\|^2.$$

This result will be needed later in the paper, when the a posteriori estimator is derived.

The following technical result available in [11] states that, since the numerical method is spurious free, for h small enough, except for κ_h , the rest of the eigenvalues of Problem 3.1 are well separated from κ .

PROPOSITION 3.12. *Let us enumerate the eigenvalues of Problem 2.1 and Problem 3.1 in increasing order as follows: $0 < \kappa_1 \leq \dots \leq \kappa_i \leq \dots$ and $0 < \kappa_{h,1} \leq \dots \leq \kappa_{h,i} \leq \dots$. Let us assume that κ_J is a simple eigenvalue of Problem 3.1. Then, there exists $h_0 > 0$ such that*

$$|\kappa_J - \kappa_{h,i}| \geq \frac{1}{2} \min_{j \neq J} |\kappa_j - \kappa_J| \quad \forall i \leq \dim \mathbf{H}_h, \quad i \neq J, \quad \forall h < h_0.$$

On the other hand, a correct control of the error $\|\mathbf{u} - \mathbf{u}_h\|_{0,\Omega}$ will be needed for the a posteriori error analysis. In order to obtain such a bound for the error, we proceed as is customary, by means of a duality argument. To perform this analysis, we adapt the arguments presented in [5] for the Stokes problem.

LEMMA 3.13. *Given $\mathbf{f} \in L^2(\Omega)^n$, let $(\tilde{\mathbf{u}}, \tilde{\boldsymbol{\omega}}, \tilde{p}) \in H_0^1(\Omega)^n \times L^2(\Omega)^{n(n-1)/2} \times L^2(\Omega)$ be the solution of (2.5) and $(\tilde{\mathbf{u}}_h, \tilde{\boldsymbol{\omega}}_h, \tilde{p}_h) \in \mathbf{H}_h \times \mathbf{Z}_h \times Q_h$ be its finite element approximation, given as the solution of (3.1). Then, there exists a positive constant C_{μ_s} such that*

$$\|\tilde{\mathbf{u}} - \tilde{\mathbf{u}}_h\|_{0,\Omega} \leq C_{\mu_s} h^s \|(\tilde{\mathbf{u}} - \tilde{\mathbf{u}}_h, \tilde{\boldsymbol{\omega}} - \tilde{\boldsymbol{\omega}}_h, \tilde{p} - \tilde{p}_h)\|.$$

Proof. Let us consider the following well posed problem, with source term $\tilde{\mathbf{u}} - \tilde{\mathbf{u}}_h$: find $(\mathbf{z}, \boldsymbol{\xi}, \phi) \in H_0^1(\Omega)^n \times L^2(\Omega)^{n(n-1)/2} \times L^2(\Omega)$ such that

$$\begin{cases} a((\boldsymbol{\theta}, q), (\boldsymbol{\xi}, \phi)) + b((\boldsymbol{\theta}, q), \mathbf{z}) &= 0 & \forall (\boldsymbol{\theta}, q) \in L^2(\Omega)^{n(n-1)/2} \times L^2(\Omega), \\ b((\boldsymbol{\xi}, \phi), \mathbf{v}) &= (\tilde{\mathbf{u}} - \tilde{\mathbf{u}}_h, \mathbf{v}) & \forall \mathbf{v} \in H^1(\Omega)^n, \end{cases}$$

where the solution satisfies

$$\|\mathbf{z}\|_{1+s,\Omega} + \|\boldsymbol{\xi}\|_{s,\Omega} + \|\phi\|_{s,\Omega} \leq C \|\tilde{\mathbf{u}} - \tilde{\mathbf{u}}_h\|_{0,\Omega},$$

with C being a generic positive constant. On the other hand, we have

$$\begin{aligned} (3.3) \quad & \|\tilde{\mathbf{u}} - \tilde{\mathbf{u}}_h\|_{0,\Omega}^2 = b((\boldsymbol{\xi}, \phi), \tilde{\mathbf{u}} - \tilde{\mathbf{u}}_h) = b((\boldsymbol{\xi} - \boldsymbol{\xi}_h, \phi - \phi_h), \tilde{\mathbf{u}} - \tilde{\mathbf{u}}_h) + b((\boldsymbol{\xi}_h, \phi_h), \tilde{\mathbf{u}} - \tilde{\mathbf{u}}_h) \\ & = b((\boldsymbol{\xi} - \boldsymbol{\xi}_h, \phi - \phi_h), \tilde{\mathbf{u}} - \tilde{\mathbf{u}}_h) + a((\tilde{\boldsymbol{\omega}} - \tilde{\boldsymbol{\omega}}_h, \tilde{p} - \tilde{p}_h), (\boldsymbol{\xi} - \boldsymbol{\xi}_h, \phi - \phi_h)) \\ & \quad - b((\tilde{\boldsymbol{\omega}} - \tilde{\boldsymbol{\omega}}_h, \tilde{p} - \tilde{p}_h), \mathbf{z} - \mathbf{z}_h) \\ & = \int_{\Omega} \operatorname{div}(\tilde{\mathbf{u}} - \tilde{\mathbf{u}}_h)(\phi - \phi_h) - \sqrt{\mu_s} \int_{\Omega} (\boldsymbol{\xi} - \boldsymbol{\xi}_h) \cdot \operatorname{curl}(\tilde{\mathbf{u}} - \tilde{\mathbf{u}}_h) - \int_{\Omega} \operatorname{div}(\mathbf{z} - \mathbf{z}_h)(\tilde{p} - \tilde{p}_h) \\ & + \sqrt{\mu_s} \int_{\Omega} (\tilde{\boldsymbol{\omega}} - \tilde{\boldsymbol{\omega}}_h) \cdot \operatorname{curl}(\mathbf{z} - \mathbf{z}_h) + \int_{\Omega} (\tilde{\boldsymbol{\omega}} - \tilde{\boldsymbol{\omega}}_h) \cdot (\boldsymbol{\xi} - \boldsymbol{\xi}_h) + (2\mu_s + \lambda_s)^{-1} \int_{\Omega} (\tilde{p} - \tilde{p}_h)(\phi - \phi_h). \end{aligned}$$

At this point, we recall the decompositions $\tilde{p} = \tilde{p}_0 + P_m \tilde{p}$ and $\tilde{p}_h = \tilde{p}_{0,h} + P_m \tilde{p}_{0,h}$ which, together with an integration by parts, reveal that

$$(3.4) \quad - \int_{\Omega} \operatorname{div}(\mathbf{z} - \mathbf{z}_h)(\tilde{p} - \tilde{p}_h) = - \int_{\Omega} \operatorname{div}(\mathbf{z} - \mathbf{z}_h)(\tilde{p}_0 - \tilde{p}_{0,h}).$$

Hence, replacing (3.4) in (3.3), applying Cauchy-Schwarz inequality, approximation errors, multiplying and dividing by $\sqrt{\mu_s}$, and using the definition of $\|\cdot\|$, we obtain

$$\|\tilde{\mathbf{u}} - \tilde{\mathbf{u}}_h\|_{0,\Omega}^2 \leq C_{\mu_s} h^s \|(\tilde{\boldsymbol{\omega}} - \tilde{\boldsymbol{\omega}}_h, \tilde{p} - \tilde{p}_h, \tilde{\mathbf{u}} - \tilde{\mathbf{u}}_h)\| \|\tilde{\mathbf{u}} - \tilde{\mathbf{u}}_h\|_{0,\Omega},$$

which concludes the proof. \square

With the above result at hand, we are allowed to define the following operators: for any $\mathbf{f} \in L^2(\Omega)^n$ we introduce the linear and compact operator $\hat{\mathbf{T}}$ defined by

$$\hat{\mathbf{T}} : L^2(\Omega)^n \rightarrow L^2(\Omega)^n, \quad \mathbf{f} \mapsto \hat{\mathbf{T}} \mathbf{f} := \tilde{\mathbf{u}}_h,$$

where the triplet $(\tilde{\mathbf{u}}, \tilde{\boldsymbol{\omega}}, \tilde{p})$ is the solution of (2.5). Also, we introduce $\hat{\mathbf{T}}_h$ as the discrete linear counterpart of $\hat{\mathbf{T}}$, defined by

$$\hat{\mathbf{T}}_h : L^2(\Omega)^n \rightarrow \mathbf{H}_h, \quad \mathbf{f} \mapsto \hat{\mathbf{T}}_h \mathbf{f} := \tilde{\mathbf{u}}_h,$$

where the triplet $(\tilde{\mathbf{u}}_h, \tilde{\boldsymbol{\omega}}_h, \tilde{p}_h)$ is the solution of (3.1). It is easy to check that the operators $\hat{\mathbf{T}}$ and $\hat{\mathbf{T}}_h$ are self-adjoint with respect to the $L^2(\Omega)$ inner product.

Therefore, thanks to Corollary 3.2 and Lemma 3.13, we guarantee the convergence in norm of $\widehat{\mathbf{T}}_h$ to $\widehat{\mathbf{T}}$ as $h \rightarrow 0$, i.e.

$$(3.5) \quad \|\widetilde{\mathbf{u}} - \widetilde{\mathbf{u}}_h\|_{0,\Omega} \leq C_{\mu_s} h^s \|\widetilde{\mathbf{u}} - \widetilde{\mathbf{u}}_h, \widetilde{\boldsymbol{\omega}} - \widetilde{\boldsymbol{\omega}}_h, \widetilde{p} - \widetilde{p}_h\| \leq C_{\mu_s} h^{2s}.$$

Since we have the convergence of $\widehat{\mathbf{T}}_h$ to $\widehat{\mathbf{T}}$ as $h \rightarrow 0$, the compactness of $\widehat{\mathbf{T}}$ and using the fact that $\widehat{\mathbf{T}}$ is selfadjoint with respect to the L^2 product, we conclude, as we already proved in Corollary 3.2 for the H^1 norm, that the eigenfunctions converge also in L^2 norm. Then we have proved the following result.

LEMMA 3.14. *Let $(\kappa_h, \mathbf{u}_h, \boldsymbol{\omega}_h, p_h)$ be the solution of Problem 3.1 with $\|\mathbf{u}_h\|_{0,\Omega} = 1$. There exists a solution $(\kappa, \mathbf{u}, \boldsymbol{\omega}, p)$ of Problem 2.1 with $\|\mathbf{u}\|_{0,\Omega} = 1$, such that $\kappa_h \rightarrow \kappa$. Moreover, there exists $C_{\mu_s} > 0$ such that*

$$\|\mathbf{u} - \mathbf{u}_h\|_{0,\Omega} \leq C_{\mu_s} h^{2s},$$

where $s \in (0, \widehat{s})$ as in Lemma 2.3.

Now, with all the ingredients at hand, we are in a position to establish a reliable and efficient a posteriori estimator of low order.

3.4. A posteriori error analysis. The following section is dedicated to the design and analysis of an a posteriori error estimator for our mixed eigenvalue problem. Let us remark that for simplicity, we consider eigenvalues with simple multiplicity. Also, the numerical analysis of the a posteriori error estimator will be for the lowest order of approximation.

Let $\mathbf{I}_h : H^1(\Omega)^n \rightarrow \mathbf{H}_h$, be the Scott-Zhang interpolant of \mathbf{u} . The following lemma establishes the local approximation properties of \mathbf{I}_h (see [26]).

LEMMA 3.15. *There exist constants $c_1, c_2 > 0$, independent of h , such that for all $\mathbf{v} \in H^1(\Omega)^n$ there holds*

$$\|\mathbf{v} - \mathbf{I}_h \mathbf{v}\|_{0,T} \leq c_1 h_T \|\mathbf{v}\|_{1,\Delta_T} \quad \forall T \in \mathcal{T}_h,$$

and

$$\|\mathbf{v} - \mathbf{I}_h \mathbf{v}\|_{0,e} \leq c_2 h_e^{1/2} \|\mathbf{v}\|_{1,\Delta_e} \quad \forall e \in \mathcal{E}_h,$$

where $\Delta_T := \{T' \in \mathcal{T}_h : T' \text{ and } T \text{ share an edge}\}$ and $\Delta_e := \cup\{T' \in \mathcal{T}_h : e \in \mathcal{E}(T')\}$.

3.5. The local and global error indicators. Now we present the local indicator associated to our spectral problem. The proposed local indicator is defined as follows

$$\begin{aligned} \zeta_T^2 := & \frac{h_T^2}{\mu_s} \|\kappa_h \mathbf{u}_h - \nabla p_h - \sqrt{\mu_s} \mathbf{curl} \boldsymbol{\omega}_h\|_{0,T}^2 + \|\sqrt{\mu_s} \mathbf{curl} \mathbf{u}_h - \boldsymbol{\omega}_h\|_{0,T}^2 \\ & + \frac{\mu_s(2\mu_s + \lambda_s)}{3\mu_s + \lambda_s} \|(2\mu_s + \lambda_s)^{-1} p_h + \operatorname{div} \mathbf{u}_h\|_{0,T}^2 + \sum_{e \in \partial T} \frac{h_e}{\mu_s} \|\mathbf{J}_e\|_{0,\partial T}^2, \end{aligned}$$

where

$$\mathbf{J}_e := \begin{cases} \frac{1}{2} [p_h \mathbf{n} + \sqrt{\mu_s} \boldsymbol{\omega}_h \times \mathbf{n}], & e \in \mathcal{E}_h(\Omega), \\ \mathbf{0}, & e \in \mathcal{E}_h(\partial\Omega). \end{cases}$$

and hence, the a posteriori error estimator is

$$(3.6) \quad \zeta := \left(\sum_{T \in \mathcal{T}_h} \zeta_T^2 \right)^{1/2}.$$

Now the study focus in the analysis of ζ , where the aim is to prove that the proposed estimator is equivalent with the approximation error of the eigenfunctions. More precisely, as is customary in a posteriori analysis, the task is to prove that the estimator ζ is reliable and efficient. We begin with the reliability bound.

3.6. Reliability. The goal of this section is to derive a global reliability bound for our proposed estimator defined in (3.6). This is contained in the following result.

THEOREM 3.16. *There exists a constant $C > 0$ independent of h such that*

$$\|(\mathbf{u} - \mathbf{u}_h, \boldsymbol{\omega} - \boldsymbol{\omega}_h, p - p_h)\| \leq C \left(\zeta + \frac{1}{\sqrt{\mu_s}} |\kappa - \kappa_h| + \frac{|\kappa|}{\sqrt{\mu_s}} \|\mathbf{u} - \mathbf{u}_h\|_{0,\Omega} \right).$$

Proof. Since $(\kappa, \mathbf{u}, \boldsymbol{\omega}, p) \in \mathbf{H}_0^1(\Omega)^n \times \mathbf{L}^2(\Omega)^{n(n-1)/2} \times \mathbf{L}^2(\Omega)$ is the solution of Problem 2.1 and $(\kappa_h, \mathbf{u}_h, \boldsymbol{\omega}_h, p_h) \in \mathbf{H}_h \times \mathbf{Z}_h \times Q_h$ is the solution of Problem 3.1, we have:

$$\mathcal{A}((\mathbf{u} - \mathbf{u}_h, \boldsymbol{\omega} - \boldsymbol{\omega}_h, p - p_h), (\mathbf{v}_h, \mathbf{0}, 0)) = (\kappa_h \mathbf{u}_h - \kappa \mathbf{u}, \mathbf{v}_h),$$

where \mathbf{v}_h is the Scott-Zhang interpolant of \mathbf{v} . Let us define the error by $\mathbf{e} := (\mathbf{u} - \mathbf{u}_h, \boldsymbol{\omega} - \boldsymbol{\omega}_h, p - p_h) \in \mathbf{H}_0^1(\Omega)^n \times \mathbf{L}^2(\Omega)^{n(n-1)/2} \times \mathbf{L}^2(\Omega)$ and let $\|(\mathbf{v} - \mathbf{v}_h, \boldsymbol{\theta}, q)\| \leq C \|\mathbf{e}\|$. Then, by Lemma 2.2 and the previous estimate, it follows that

$$\begin{aligned} C \|\mathbf{e}\|^2 &\leq \mathcal{A}(\mathbf{e}, (\mathbf{v}, \boldsymbol{\theta}, q)) = \mathcal{A}(\mathbf{e}, (\mathbf{v} - \mathbf{v}_h, \boldsymbol{\theta}, q)) + \mathcal{A}(\mathbf{e}, (\mathbf{v}_h, \mathbf{0}, 0)) \\ &= \kappa_h (\mathbf{u}_h, \mathbf{v}_h) - \kappa (\mathbf{u}, \mathbf{v}) - \mathcal{A}((\mathbf{u}_h, \boldsymbol{\omega}_h, p_h), (\mathbf{v} - \mathbf{v}_h, \boldsymbol{\theta}, q)) \\ &= \kappa_h (\mathbf{u}_h, \mathbf{v}_h - \mathbf{v}) + (\kappa_h - \kappa) (\mathbf{u}_h, \mathbf{v}) + \kappa (\mathbf{u}_h - \mathbf{u}, \mathbf{v}_h) - \mathcal{A}((\mathbf{u}_h, \boldsymbol{\omega}_h, p_h), (\mathbf{v} - \mathbf{v}_h, \boldsymbol{\theta}, q)) \\ &= (\kappa_h - \kappa) (\mathbf{u}_h, \mathbf{v}) + \kappa (\mathbf{u}_h - \mathbf{u}, \mathbf{v}_h) + \int_{\Omega} (\sqrt{\mu_s} \mathbf{curl} \mathbf{u}_h - \boldsymbol{\omega}_h) \cdot \boldsymbol{\theta} \\ &\quad - \int_{\Omega} ((2\mu_s + \lambda_s)^{-1} p_h + \operatorname{div} \mathbf{u}_h) q + \sum_{T \in \mathcal{T}_h} \left(\kappa_h \int_T \mathbf{u}_h \cdot (\mathbf{v}_h - \mathbf{v}) - \int_T \operatorname{div}(\mathbf{v} - \mathbf{v}_h) p_h \right. \\ &\quad \left. + \int_T \sqrt{\mu_s} \boldsymbol{\omega}_h \cdot \mathbf{curl}(\mathbf{v} - \mathbf{v}_h) \right) \\ &\leq C \left(\frac{1}{\sqrt{\mu_s}} (|\kappa_h - \kappa| + \frac{|\kappa|}{\sqrt{\mu_s}} \|\mathbf{u}_h - \mathbf{u}\|_{0,\Omega}) + \zeta \right) \|(\mathbf{v}, \boldsymbol{\theta}, q)\|. \end{aligned}$$

The proof is concluded using the fact that $\|(\mathbf{v} - \mathbf{v}_h, \boldsymbol{\theta}, q)\| \leq C \|\mathbf{e}\|$. \square

Now, from Remark 3.11, Theorem 3.16, and in view of Lemma 3.14, the terms $|\kappa - \kappa_h|$ and $\|\mathbf{u} - \mathbf{u}_h\|_{0,\Omega}$ are high order terms and so, we deduce the following reliability result for ζ .

COROLLARY 3.17. *There exists a constant $C_{1,\mu_s} > 0$ independent of h such that, for all $h < h_0$, there holds*

$$\|(\mathbf{u} - \mathbf{u}_h, \boldsymbol{\omega} - \boldsymbol{\omega}_h, p - p_h)\| \leq C_{1,\mu_s} (\zeta + h^{2s}).$$

Moreover, there exists a constant $C_{2,\mu_s} >$ such that

$$|\kappa - \kappa_h| \leq C_{2,\mu_s} (\zeta^2 + h^{4s}).$$

3.7. Efficiency. In this section we analyze the efficiency for the proposed estimator ζ . To do this task, we introduce some technical preliminaries. We begin by introducing the bubble functions for two dimensional elements. Given $T \in \mathcal{T}_h$ and $e \in \mathcal{E}(T)$, we let ψ_T and ψ_e be the usual triangle-bubble and edge-bubble functions, respectively (see [28] for further details about these functions), which satisfy the following properties

1. $\psi_T \in \mathbb{P}_\ell(T)$, with $\ell = 3$ for 2D or $\ell = 4$ for 3D, $\text{supp}(\psi_T) \subset T$, $\psi_T = 0$ on ∂T and $0 \leq \psi_T \leq 1$ in T ;
2. $\psi_e|_T \in \mathbb{P}_\ell(T)$, with $\ell = 2$ for 2D or $\ell = 3$ for 3D, $\text{supp}(\psi_e) \subset \omega_e := \cup\{T' \in \mathcal{T}_h : e \in \mathcal{E}(T')\}$, $\psi_e = 0$ on $\partial T \setminus e$ and $0 \leq \psi_e \leq 1$ in ω_e .

The following properties, proved in [27, Lemma 1.3] for an arbitrary polynomial order of approximation, hold.

LEMMA 3.18 (Bubble function properties). *Given $\ell \in \mathbb{N} \cup \{0\}$, and for each $T \in \mathcal{T}_h$ and $e \in \mathcal{E}(T)$, there following estimates hold*

$$\begin{aligned} \|\psi_T q\|_{0,T}^2 &\leq \|q\|_{0,T}^2 \leq C \|\psi_T^{1/2} q\|_{0,T}^2 \quad \forall q \in \mathbb{P}_\ell(T), \\ \|\psi_e L(p)\|_{0,e}^2 &\leq \|p\|_{0,e}^2 \leq C \|\psi_e^{1/2} p\|_{0,e}^2 \quad \forall p \in \mathbb{P}_\ell(e), \end{aligned}$$

and

$$h_e \|p\|_{0,e}^2 \leq C \|\psi_e^{1/2} L(p)\|_{0,T}^2 \leq C h_e \|p\|_{0,e}^2 \quad \forall p \in \mathbb{P}_\ell(e),$$

where L is the extension operator defined by $L : \mathcal{C}(e) \rightarrow \mathcal{C}(T)$ with $\mathcal{C}(e)$ and $\mathcal{C}(T)$ being the spaces of continuous functions defined on e and T , respectively, and satisfying $L(p) \in \mathbb{P}_k(T)$ and $L(p)|_e = p$ for all $p \in \mathbb{P}_k(e)$, where the hidden constants depend on k and the shape regularity of the triangulation.

Also, we require the following technical result (see [13, Theorem 3.2.6]).

LEMMA 3.19 (Inverse inequality). *Let $l, m \in \mathbb{N} \cup \{0\}$ such that $l \leq m$. Then, for each $T \in \mathcal{T}_h$ there holds*

$$|q|_{m,T} \leq C h_T^{l-m} |q|_{l,T} \quad \forall q \in \mathbb{P}_k(T),$$

where the hidden constant depends on k, l, m and the shape regularity of the triangulations.

Now our task is to prove the efficiency. In order to simplify the presentation of the material, we define $\mathbf{R}_1 := (\kappa_h \mathbf{u}_h - \nabla p_h - \sqrt{\mu_s} \mathbf{curl} \boldsymbol{\omega}_h)|_T$ and $\boldsymbol{\chi}|_T := (\mu_s)^{-1} h_T^2 \mathbf{R}_1 \psi_T$, where ψ_T is the bubble function defined in Lemma 3.18. Then, we have

$$(3.7) \quad (\mu_s)^{-1} h_T^2 \|\mathbf{R}_1\|_{0,T}^2 \leq C \int_T \mathbf{R}_1 \cdot \boldsymbol{\chi}.$$

From the first equation of (2.2) we have that $\kappa \mathbf{u} - \sqrt{\mu_s} \mathbf{curl} \boldsymbol{\omega} - \nabla p = 0$ in Ω . Then, using this in (3.7) we have

$$\begin{aligned} (3.8) \quad C^{-1} (\mu_s)^{-1} h_T^2 \|\mathbf{R}_1\|_{0,T}^2 &\leq \int_T \mathbf{R}_1 \cdot \boldsymbol{\chi} = \int_T (\kappa_h \mathbf{u}_h - \kappa \mathbf{u}) \cdot \boldsymbol{\chi} \\ &\quad + \sqrt{\mu_s} \int_T \mathbf{curl}(\boldsymbol{\omega} - \boldsymbol{\omega}_h) \cdot \boldsymbol{\chi} + \int_T \nabla(p - p_h) \cdot \boldsymbol{\chi} \\ &= C \int_T (\kappa_h \mathbf{u}_h - \kappa \mathbf{u}) \cdot \boldsymbol{\chi} + \sqrt{\mu_s} \int_T (\boldsymbol{\omega} - \boldsymbol{\omega}_h) \cdot \mathbf{curl} \boldsymbol{\chi} + \int_T (p - p_h) \text{div} \boldsymbol{\chi} \\ &\leq ((\mu_s)^{-1/2} h_T \|\kappa_h \mathbf{u}_h - \kappa \mathbf{u}\|_{0,T} + \mu_s^{-1/2} \|p - p_h\|_{0,T} \\ &\quad + \|\boldsymbol{\omega} - \boldsymbol{\omega}_h\|_{0,T}) (\mu_s^{1/2} \|\nabla \boldsymbol{\chi}\|_{0,T} + \mu_s^{1/2} h_T^{-1} \|\boldsymbol{\chi}\|_{0,T}). \end{aligned}$$

Note that the following estimate holds

$$\mu_s^{1/2}(\|\nabla \boldsymbol{\chi}\|_{0,T} + h_T^{-1}\|\boldsymbol{\chi}\|_{0,T}) \leq \mu^{-1/2}h_T\|\mathbf{R}_1\|_{0,T},$$

which we replace in (3.8) in order to obtain

$$(3.9) \quad h_T(\mu_s)^{-1/2}\|\mathbf{R}_1\|_{0,T} \leq C(h_T(\mu_s)^{-1/2}\|\kappa_h \mathbf{u}_h - \kappa \mathbf{u}\|_{0,T} + (\mu_s)^{-1/2}\|p - p_h\|_{0,T} + \|\boldsymbol{\omega} - \boldsymbol{\omega}_h\|_{0,T}).$$

Now we define the quantities $\mathbf{R}_2 := (\sqrt{\mu_s} \mathbf{curl} \mathbf{u}_h - \boldsymbol{\omega}_h)|_T$ and $\mathbf{R}_3 := ((2\mu_s + \lambda_s)^{-1}p_h + \operatorname{div} \mathbf{u}_h)|_T$. Then, from [4, Lemma 2.2] and [4, Lemma 2.3], respectively, we have

$$(3.10) \quad \|\mathbf{R}_2\|_{0,T} \lesssim \|\boldsymbol{\omega} - \boldsymbol{\omega}_h\|_{0,T} + \sqrt{\mu_s}\|\mathbf{curl}(\mathbf{u} - \mathbf{u}_h)\|_{0,T}.$$

and

$$(3.11) \quad (\mu_s^{-1} + (2\mu_s + \lambda_s)^{-1})^{-1/2}\|\mathbf{R}_3\|_{0,T} \lesssim \sqrt{\mu}\|\operatorname{div}(\mathbf{u} - \mathbf{u}_h)\|_{0,T} + (2\mu_s + \lambda_s)^{-1/2}\|p - p_h\|_{0,T}.$$

Similarly, proceeding as in [4, lemma 2.4] we can prove the following property

$$(3.12) \quad h_e^{1/2}(\mu_s)^{-1/2}\|\mathbf{J}_e\|_{0,e} \leq C\left(\sum_{T \in \omega_e} h_T(\mu_s)^{-1/2}\|\mathbf{R}_1\|_{0,T} + h_T(\mu_s)^{-1/2}\|\kappa_h \mathbf{u}_h - \kappa \mathbf{u}\|_{0,T} + (\mu_s)^{-1/2}\|p - p_h\|_{0,T} + \|\boldsymbol{\omega} - \boldsymbol{\omega}_h\|_{0,T}\right).$$

Finally, gathering (3.9), (3.10), (3.11), and (3.12), we have the following result, which allows us to deduce the efficiency of the error indicator up to higher order terms.

THEOREM 3.20 (Efficiency). *Let $(\mathbf{u}, \boldsymbol{\omega}, p)$ be the solution to Problem 2.1 and let $(\mathbf{u}_h, \boldsymbol{\omega}_h, p_h)$ be its finite element approximation, given as the solution to Problem 3.1. Then we have*

$$\zeta \leq C(\|(\mathbf{u} - \mathbf{u}_h, \boldsymbol{\omega} - \boldsymbol{\omega}_h, p - p_h)\| + h^{2s+1}),$$

where $C > 0$ and is independent of h , λ_s and the discrete solution.

Proof. From (3.9)–(3.12) we have

$$\zeta \leq C(\|(\mathbf{u} - \mathbf{u}_h, \boldsymbol{\omega} - \boldsymbol{\omega}_h, p - p_h)\| + h(\mu_s)^{-1/2}\|\kappa_h \mathbf{u}_h - \kappa \mathbf{u}\|_{0,\Omega}).$$

Observe that, using the fact $\|\mathbf{u}\|_{0,\Omega} = 1$, we have $\|\kappa \mathbf{u} - \kappa_h \mathbf{u}_h\|_{0,\Omega}^2 \leq 2(\kappa^2\|\mathbf{u} - \mathbf{u}_h\|_{0,\Omega}^2 + |\kappa - \kappa_h|^2)$. Hence

$$\zeta \leq C(\|(\mathbf{u} - \mathbf{u}_h, \boldsymbol{\omega} - \boldsymbol{\omega}_h, p - p_h)\| + h^{2s+1}).$$

4. Numerical experiments. In this section we report some numerical tests in order to assess the performance of the proposed mixed finite element method. Some of the meshes used in this work were constructed using the meshing software Gmsh [16]. The numerical scheme have been implemented in a FEniCS script [2], where the results of the convergence rates associated to the a priori analysis and the a posteriori error estimator were obtained. More precisely, the convergence rates of the eigenvalues have been obtained with a standard least square fitting and highly refined meshes.

We denote by κ_{h_i} the i -th lowest computed eigenvalue, whereas κ_{extr} or κ_i denotes the corresponding extrapolated eigenvalue. Note that the square root of this values gives the corresponding eigenfrequency. We also denote by N the mesh refinement level, whereas \mathbf{dof} denotes the number of degrees of freedom.

Hence, we denote the error on the i -th eigenfrequency by $\mathbf{err}(\kappa_i)$ with

$$\mathbf{err}(\kappa_i) := |\sqrt{\kappa_{h_i}} - \sqrt{\kappa_i}|.$$

For the computation of order of convergence, in two-dimensional geometries, we consider polynomial degrees $k = 1, 2, 3$, whereas for three-dimensional cases we consider only the lowest order $k = 1$ due to machine memory limitations.

Let us remark that, when the Poisson ratio is too close to $1/2$, the numerical method loses stability, which is reflected in the convergence order of approximation of the eigenvalues. To remedy this problem, an option is to stabilize the method, adding a term that compensates the presence of $p_{0,h}$ for the nearly incompressible case (see [18, Section 3]). This stabilization, which we add to Problem 3.1 is as follows

$$(4.1) \quad \mathcal{A}((\mathbf{u}_h, \boldsymbol{\omega}_h, p_h), (\mathbf{v}_h, \boldsymbol{\theta}_h, q_h)) + \alpha^{-1} \sum_{e \in \mathcal{E}_h(\Omega)} h_e \int_e \llbracket p \rrbracket \llbracket q \rrbracket = -\kappa_h(\mathbf{u}_h, \mathbf{v}_h)_{0,\Omega}.$$

The value of α is conditioned by the value of ν , so that the stabilization gets relevant when $\nu \approx 0.5$. As in Section 3.3, the arguments of the continuous problem allow us to conclude that (4.1) is well-posed, and therefore we have the respective discrete estimates for the source problem. The stabilization parameter for the limiting case can take different values. In our work, we will consider those values such that the convergence of the experiment can be captured in low and high order discontinuous pressure elements (see, for example, [18, Remark 3]).

4.1. A priori numerical experiments. In this section we present experiments using uniform meshes in order to study the convergence of the method in the compressible and quasi-incompressible cases. The experiments that we report are performed in two and three dimensions, using different polynomial degrees.

4.1.1. Test 1: Square domain. In this experiment we consider the unit square $\Omega := (0, 1)^2$ with boundary conditions $\mathbf{u} = 0$ over the entire domain. An example of the used for this experiment is depicted in Figure 1. The mesh refinement level on this mesh is such that the number of elements is asymptotically $2N^2$. The Poisson's coefficient is taken as $\nu \in \{0.35, 0.49, 0.499, 0.4999\}$.

Table 1 show the convergence behavior when we consider different values of ν for the lowest order polynomial approximation. It notes that the convergence order remains optimal when ν approaches to the incompressibility limit. Values of ν closer to 0.5 than the ones showed here gave similar result. We also considered higher order polynomials for the near incompressible case, whose behavior is depicted in Figure 2 for $\nu = 0.4999$. It is clear that $|\sqrt{\kappa_h} - \sqrt{\kappa_{extr}}| \approx \mathcal{O}(\mathbf{dof}^{-k}) \approx \mathcal{O}(h^{2k})$. The noise in the curves for $k = 3$ are produced by the closeness between the computed eigenvalues and the extrapolated values, together with round-off error.

4.1.2. Test 2: Torus domain. This test focus on a three dimensional non-polygonal domain. We consider a torus azimuthally symmetric about the z -axis, whose domain is characterized by

$$\Omega := \left\{ (x, y, z) \in \mathbb{R}^3 : \left(\sqrt{x^2 + y^2} - R \right)^2 + z^2 = r^2 \right\},$$

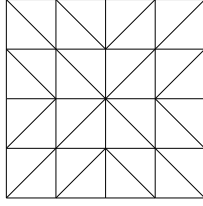
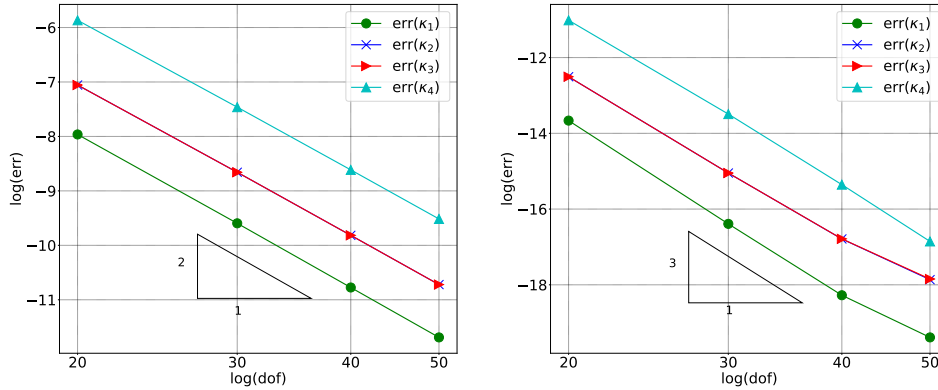
FIG. 1. Test 1. Sample mesh of the unit square $\Omega = (0, 1)^2$, with $N = 4$.

TABLE 1

Test 1. Lowest computed eigenvalues for polynomial degree $k = 1$ and different values of ν .

| ν | $N = 20$ | $N = 30$ | $N = 40$ | $N = 50$ | Order | $\sqrt{\kappa_{extr}}$ |
|--------|----------|----------|----------|----------|-------|------------------------|
| 0.35 | 4.21034 | 4.20058 | 4.19725 | 4.19573 | 2.10 | 4.19317 |
| | 4.21034 | 4.20058 | 4.19725 | 4.19573 | 2.11 | 4.19317 |
| | 4.41054 | 4.38897 | 4.38155 | 4.37814 | 2.08 | 4.37235 |
| | 5.98625 | 5.95624 | 5.94595 | 5.94125 | 2.09 | 5.93336 |
| 0.49 | 4.24033 | 4.21090 | 4.20083 | 4.19627 | 2.08 | 4.18836 |
| | 5.62215 | 5.56252 | 5.54232 | 5.53317 | 2.07 | 5.51698 |
| | 5.62215 | 5.56252 | 5.54232 | 5.53317 | 2.07 | 5.51698 |
| | 6.76422 | 6.63819 | 6.59545 | 6.57609 | 2.08 | 6.54236 |
| 0.499 | 4.23323 | 4.20247 | 4.19176 | 4.18682 | 2.03 | 4.17803 |
| | 5.65631 | 5.59002 | 5.56741 | 5.55713 | 2.07 | 5.53911 |
| | 5.65631 | 5.59002 | 5.56741 | 5.55713 | 2.07 | 5.53911 |
| | 6.77552 | 6.64170 | 6.59562 | 6.57447 | 2.04 | 6.53699 |
| 0.4999 | 4.23261 | 4.20174 | 4.19098 | 4.18601 | 2.01 | 4.17701 |
| | 5.66107 | 5.59383 | 5.57062 | 5.55994 | 2.03 | 5.54082 |
| | 5.66107 | 5.59383 | 5.57062 | 5.55994 | 2.03 | 5.54082 |
| | 6.77726 | 6.64276 | 6.59637 | 6.57502 | 2.02 | 6.53643 |

FIG. 2. Test 1. Error curves on the incompressibility limit $\nu = 0.4999$ for $k = 2$ (left) and $k = 3$ (right).

where $R = 1/2$ and $r = 1/4$. We test the deformation, pressure and rotation with several values of ν , for which the stabilization parameter in the incompressibility case is chosen as $\alpha^{-1} = 1/8$. The refinement levels for the mesh are such that the mesh parameter is asymptotically $h = 1/N$, where $N = 30, 40, 50, 60$.

Table 2 we observe the convergence behavior for the first four lowest eigenfrequencies

cies. Since each slice of the torus is a circle, we are committing a variational crime when we discretise this domain using polygons. Hence, the convergence rate $\mathcal{O}(h^2)$ will remain for $k > 1$. In the case provided in this experiment, the optimal rate is recovered even near the incompressible limit. In Figures 3 – 5 we depict some of the eigenmodes computed in Table 2 with $N = 60$.

TABLE 2

Test 2. Lowest computed eigenvalues for the lowest order scheme $k = 1$ and different values of ν in the torus domain.

| ν | $N = 30$ | $N = 40$ | $N = 50$ | $N = 60$ | Order | $\sqrt{\kappa_{extr}}$ |
|--------|----------|----------|----------|----------|-------|------------------------|
| 0.35 | 6.04924 | 5.99800 | 5.97977 | 5.97149 | 2.13 | 5.95707 |
| | 6.43508 | 6.37877 | 6.35886 | 6.34987 | 2.16 | 6.33465 |
| | 6.43601 | 6.37934 | 6.35917 | 6.34995 | 2.20 | 6.33538 |
| | 7.39830 | 7.32671 | 7.30098 | 7.28926 | 2.19 | 7.27061 |
| 0.49 | 5.73450 | 5.69843 | 5.68588 | 5.68013 | 2.17 | 5.67049 |
| | 8.68185 | 8.60391 | 8.57378 | 8.55986 | 1.92 | 8.53153 |
| | 8.68229 | 8.60483 | 8.57428 | 8.56007 | 1.87 | 8.53011 |
| | 8.91109 | 8.73963 | 8.67989 | 8.65273 | 2.17 | 8.60686 |
| 0.4999 | 5.71598 | 5.67978 | 5.66718 | 5.66142 | 2.22 | 5.65241 |
| | 8.91911 | 8.74350 | 8.68319 | 8.65521 | 2.26 | 8.61376 |
| | 8.92069 | 8.74412 | 8.68322 | 8.65542 | 2.27 | 8.61404 |
| | 8.92674 | 8.74496 | 8.68354 | 8.65639 | 2.28 | 8.61386 |

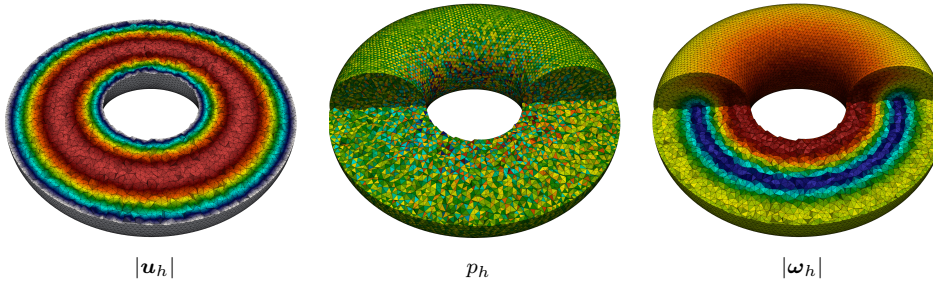


FIG. 3. Test 2. Slices of the torus domain showing the eigenmodes for the first lowest frequency, with $\nu = 0.35$.

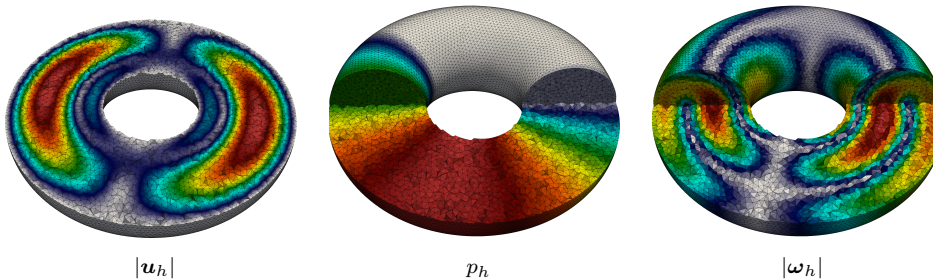


FIG. 4. Test 2. Slices of the torus domain showing the eigenmodes for the second lowest frequency, with $\nu = 0.49$.

4.2. Experiments using adaptive refinements. In this section we test our a posteriori estimator ζ , previously introduced and analyzed in Section 3.4. With the

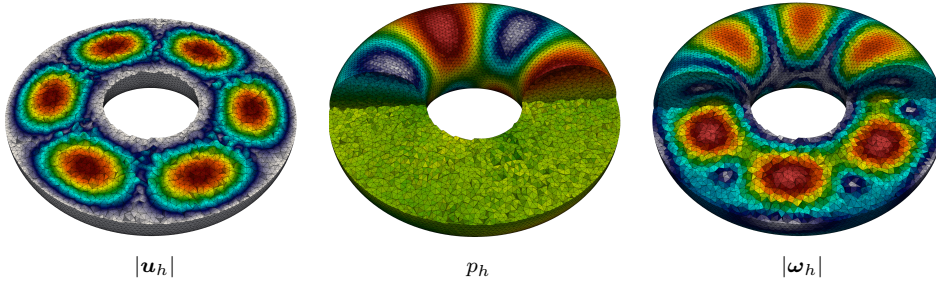


FIG. 5. *Test 2. Slices of the torus domain showing the eigenmodes for the fourth lowest frequency, with $\nu = 0.4999$.*

aim of assess the performance of our estimator, we consider domains with singularities in two and three dimensions, expecting that the estimator be capable of identify such singularities and refine adaptively. For this tests, we consider two and three dimensional domains. On each adaptive iteration, we use the blue-green marking strategy to refine each $T' \in \mathcal{T}_h$ whose indicator $\zeta_{T'}$ satisfies

$$\zeta_{T'} \geq 0.5 \max\{\zeta_T : T \in \mathcal{T}_h\},$$

The effectivity indexes with respect to ζ and the eigenvalue κ_i are defined by

$$\mathbf{eff}(\kappa_i) := \frac{\mathbf{err}(\kappa_i)}{\zeta^2}.$$

4.2.1. Test 3. A square with a hole. In this experiment we test the adaptive algorithm in a domain containing singularities. We consider the domain $\Omega = \widehat{\Omega} \setminus \widetilde{\Omega}$, where $\widehat{\Omega}$ is the unit square rotated $\pi/4$ around its centroid, whereas $\widetilde{\Omega} := (129/400, 271/400)^2$. An example of this domain is depicted in Figure 6. The stabilization parameter for the incompressible limit is taken to be $\alpha^{-1} = 10$.

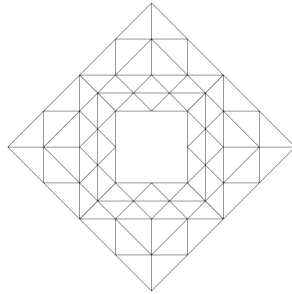


FIG. 6. *Test 3. Initial mesh on the square with a hole.*

In this case, we have 4 reentrant angles, so the first eigenfunction is singular. In fact, the optimal convergence order with uniform refinements is expected to be approximately $\mathcal{O}(N^{-\sqrt{3}/2}) \approx \mathcal{O}(h^{1.7})$ for all $k \geq 1$. To observe in detail the error behavior, we show in Figure 7 the adaptive and uniform error curves, where the rapid decay of the adaptive error is evident for $k > 1$. Moreover, in Figures 8-9 we observe that the estimator ζ^2 behaves like $\mathcal{O}(h^{2k})$, keeping the effectivity indexes appropriate bounded above and below. This verifies that our estimator is efficient and reliable.

| ν | $\sqrt{\kappa_1}$ |
|--------|-------------------|
| 0.35 | 6.14518 |
| 0.4999 | 6.04518 |

TABLE 3

Lowest computed eigenvalues obtained from highly refined meshes and least-square fitting.

The experimental convergence rate for this experiment is based on the comparison of the computed eigenvalues with the values on Table 3. On the other hand, Figures 10–11 show the meshes at different stages of the adaptive refinement for $\nu = 0.35$ and $\nu = 0.4999$, respectively. We complete this experiment by showing the first eigenmode magnitudes, together with the computed pressure and rotations, which in this case are similar for the selected values of ν . It notes that high gradients of pressure, together with high rotations are present near the singularities.

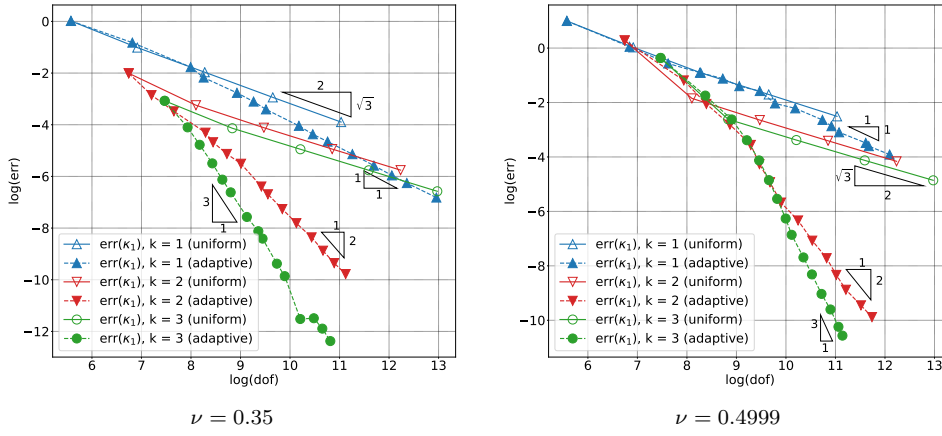


FIG. 7. Test 3. Error curves for different values of k and ν .

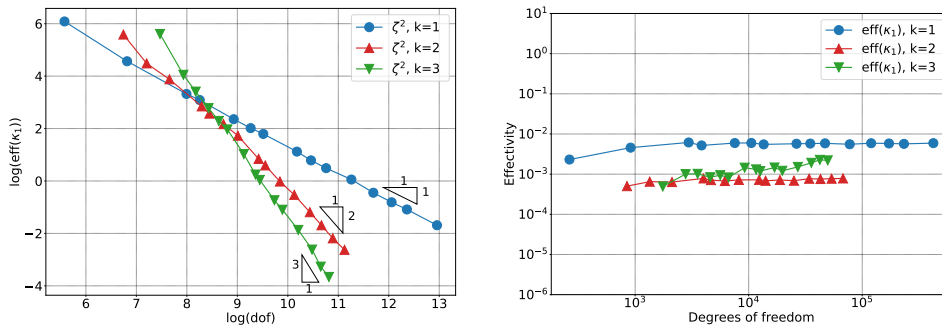


FIG. 8. Test 3. Estimator convergence and effectivity indexes for different values of k , with $\nu = 0.35$.

4.2.2. Test 4. A 3D L-shaped domain. In this experiment we consider the classical 3D L-shaped domain, which is described as

$$\Omega := (-1/2, 1/2) \times (0, 1) \times (-1/2, 1/2) \setminus ((0, 1/2) \times (0, 1) \times (0, 1/2)).$$

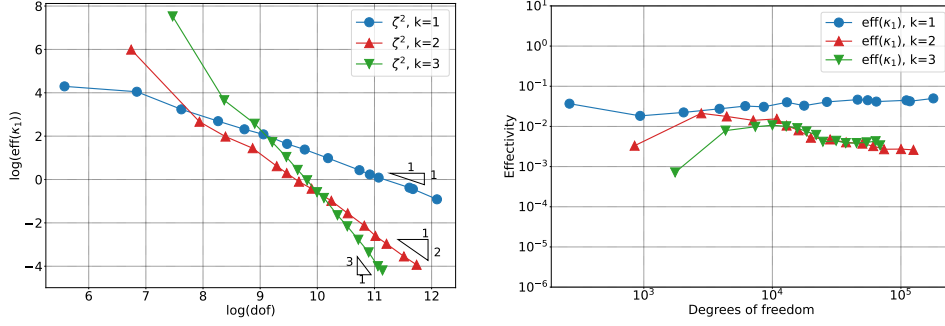


FIG. 9. Test 3. Estimator convergence and effectivity indexes for different values of k , with $\nu = 0.4999$.

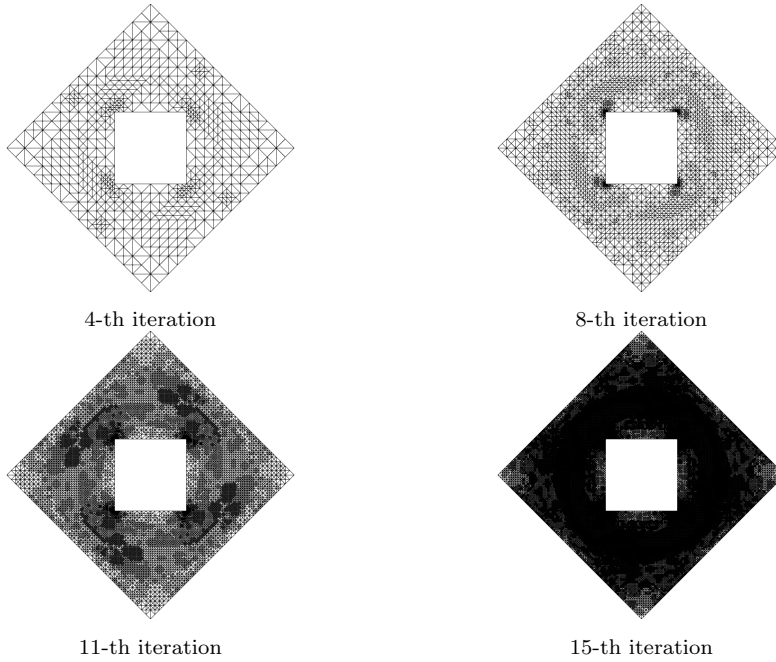


FIG. 10. Test 3. Intermediate meshes in the adaptive refinement algorithm for $k = 1$ and $\nu = 0.35$.

This domain has the characteristic of having a singularity along the line $(0, y, 0)$, for $y \in [0, 1]$, so the convergence with uniform meshes will be suboptimal. The initial mesh for this experiment is depicted in Figure 13. For the limiting case, we consider $\alpha^{-1} = 1/2$.

In Table 4 we observe the behavior of the adaptive scheme for the values of ν at the lowest polynomial order. The use of uniform meshes for this case results in an experimental convergence rate between $\mathcal{O}(\text{dof}^{-\sqrt{3}/3}) \approx \mathcal{O}(h^{1.7})$ and $\mathcal{O}(\text{dof}^{-2/3}) \approx \mathcal{O}(h^2)$, which is the best expected order for this type of refinement. The adaptive scheme in the compressible and nearly incompressible case exhibits a behavior asymptotically similar to $\mathcal{O}(h^2)$, which is the optimal order according to the theory. In Figure 14 we can observe the curve of these errors and the effectivity of our estimator, proving to be reliable and efficient. To be more precise, in Table 5 we describe the results obtained

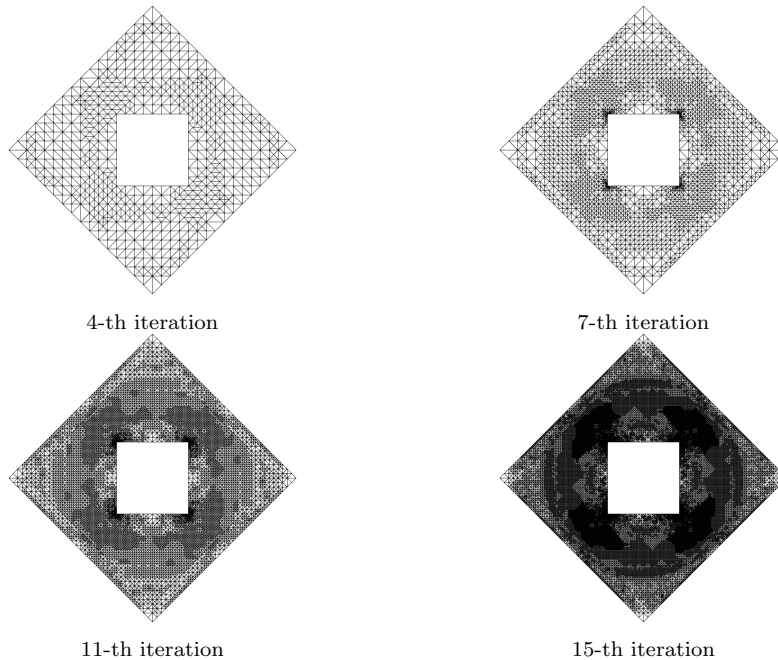


FIG. 11. *Test 3. Intermediate meshes in the adaptive refinement algorithm for $k = 1$ and $\nu = 0.4999$.*

with different values of ν , where we can observe that the errors and the estimator behave like $\mathcal{O}(h^2)$.

On the other hand, in Figure 15 we show intermediate meshes in our adaptive iterations. Note that the refinement is concentrated in the zone $(0, y, 0)$, therefore the estimator is able to detect and refine close to the singularity. To conclude, we show in Figure 16 the first eigenmode for each value of ν . The vector fields \mathbf{u}_h and \mathbf{w}_h together with their magnitudes $|\mathbf{u}_h|$ and $|\mathbf{w}_h|$, respectively, are presented in the same mesh. The pressure is represented through a surface contour plot. We note the high pressure gradients and high rotations near the singularity, as is expected.

5. Conclusions. In this paper, we have introduced an alternative formulation to study the elasticity eigenvalue problem, where the main unknowns are the displacement, rotations and pressure. More precisely, we have used this formulation to analyze a mixed finite element method, based in polynomials, to approximate the eigenvalues and associated eigenfunctions. In the a priori analysis, we have proved convergence of the proposed method and optimal order of convergence. The numerical tests, in two and three dimension, for arbitrary polynomial degrees, show two important features: in one hand, that the method is spurious free, and on the other, the stability of the numerical method when we are close to the limit case (namely $\nu = 1/2$). Also, we have proposed an a posteriori error estimator for the eigenvalue problem, that is reliable and efficient. The numerical tests that we reported show successfully that the optimal order of convergence is recovered for non smooth eigenfunctions, when the adaptive strategy is performed. Furthermore, the experiments revealed that the estimator performs an adaptive refinement that recovers the optimal order of convergence of the method. Moreover, the tests show that even for polynomial degrees $k > 1$, which are beyond the scope of the presented analysis, the estimator works correctly.

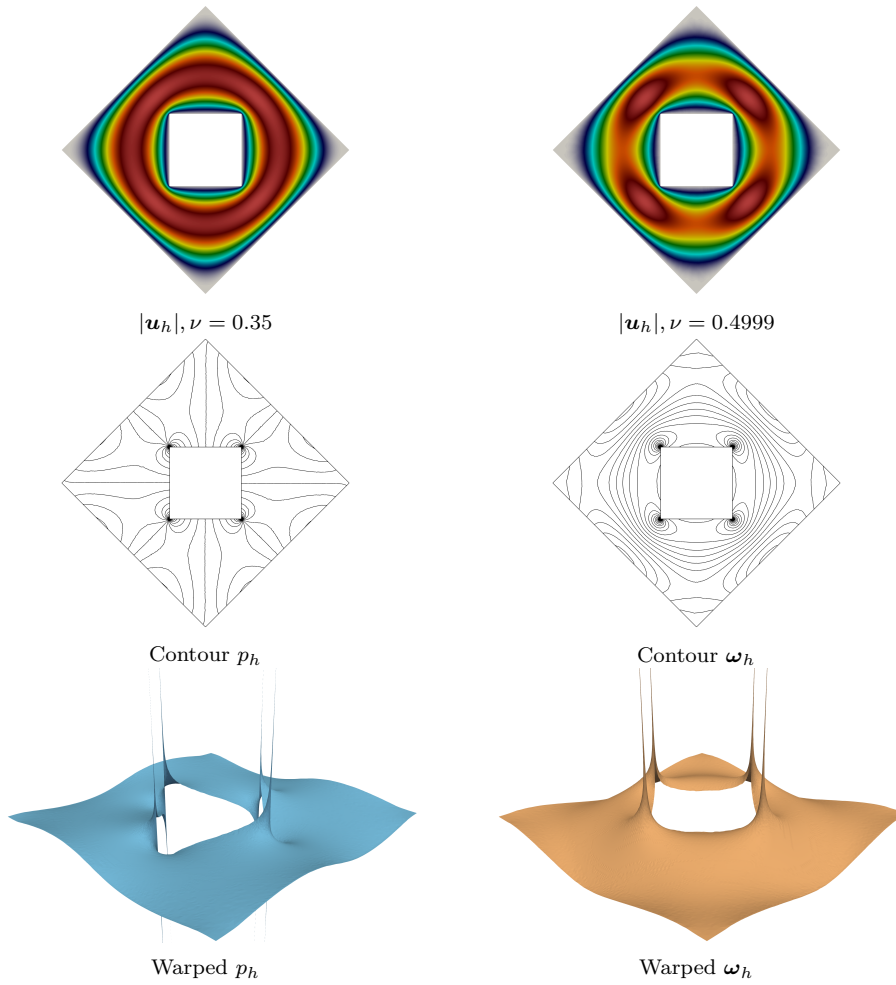


FIG. 12. *Test 3. Lowest computed eigenmodes for $k = 1$ and different values of ν . The high gradients of p_h and high rotations ω_h near the singularity for $\nu = 0.35$ and $\nu = 0.4999$ are similar.*

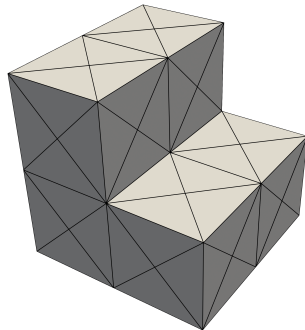


FIG. 13. *Test 4. Initial shape for the 3D L-shaped domain.*

REFERENCES

TABLE 4

Test 4: Comparison between the lowest computed eigenvalue for $k = 1$, $\nu = 0.35$ and $\nu = 0.4999$ with uniform and adaptive refinements.

| $\nu = 0.35$ | | | | $\nu = 0.4999$ | | | |
|-------------------|--------------------------|-------------------|--------------------------|-------------------|--------------------------|-------------------|--------------------------|
| Uniform | | Adaptive | | Uniform | | Adaptive | |
| dof | $\sqrt{\kappa_{h1}}$ | dof | $\sqrt{\kappa_{h1}}$ | dof | $\sqrt{\kappa_{h1}}$ | dof | $\sqrt{\kappa_{h1}}$ |
| 830 | 7.69255 | 830 | 7.69255 | 830 | 6.12221 | 830 | 6.12221 |
| 6211 | 5.76928 | 2930 | 5.97646 | 6211 | 5.78695 | 4645 | 5.77952 |
| 48347 | 5.25662 | 10132 | 5.49598 | 48347 | 5.41616 | 23289 | 5.45506 |
| 382099 | 5.10803 | 30913 | 5.28891 | 382099 | 5.28658 | 88486 | 5.34401 |
| 3039395 | 5.06572 | 68740 | 5.19462 | 3039395 | 5.25196 | 138855 | 5.31763 |
| | | 129778 | 5.14555 | | | 461939 | 5.27548 |
| | | 275240 | 5.10640 | | | 679613 | 5.26666 |
| | | 550531 | 5.08668 | | | 1690232 | 5.25403 |
| | | 882797 | 5.07516 | | | 2828623 | 5.24948 |
| | | 1849627 | 5.06375 | | | | |
| | | 1856515 | 5.06367 | | | | |
| | | 3753754 | 5.05753 | | | | |
| Order | $\mathcal{O}(N^{-0.61})$ | Order | $\mathcal{O}(N^{-0.66})$ | Order | $\mathcal{O}(N^{-0.62})$ | Order | $\mathcal{O}(N^{-0.66})$ |
| $\sqrt{\kappa_1}$ | 5.04874 | $\sqrt{\kappa_1}$ | 5.04874 | $\sqrt{\kappa_1}$ | 5.24009 | $\sqrt{\kappa_1}$ | 5.24009 |

TABLE 5

Test 4: Computed errors and effectivity indexes on the adaptively refinement meshes for $k = 1$, $\nu = 0.35$ and $\nu = 0.4999$.

| $\nu = 0.35$ | | | $\nu = 0.4999$ | | |
|---------------------------|-------------|---------------------------|---------------------------|-------------|---------------------------|
| $\text{err}(\kappa_{h1})$ | ζ^2 | $\text{eff}(\kappa_{h1})$ | $\text{err}(\kappa_{h1})$ | ζ^2 | $\text{eff}(\kappa_{h1})$ |
| 2.64380e+00 | 2.33470e+03 | 1.13239e-03 | 8.82122e-01 | 1.04890e+03 | 8.40995e-04 |
| 9.27714e-01 | 4.57985e+02 | 2.02564e-03 | 5.39432e-01 | 3.22277e+02 | 1.67381e-03 |
| 4.47229e-01 | 1.48726e+02 | 3.00707e-03 | 2.14972e-01 | 8.02553e+01 | 2.67860e-03 |
| 2.40160e-01 | 6.52344e+01 | 3.68149e-03 | 1.03919e-01 | 2.97943e+01 | 3.48787e-03 |
| 1.45869e-01 | 3.69662e+01 | 3.94601e-03 | 7.75365e-02 | 2.23126e+01 | 3.47501e-03 |
| 9.67976e-02 | 2.39336e+01 | 4.04443e-03 | 3.53827e-02 | 9.90877e+00 | 3.57084e-03 |
| 5.76481e-02 | 1.44241e+01 | 3.99665e-03 | 2.65636e-02 | 7.54860e+00 | 3.51901e-03 |
| 3.79299e-02 | 9.09617e+00 | 4.16987e-03 | 1.39398e-02 | 4.34538e+00 | 3.20796e-03 |
| 2.64066e-02 | 6.67283e+00 | 3.95733e-03 | 9.38544e-03 | 3.01470e+00 | 3.11322e-03 |
| 1.50016e-02 | 4.07549e+00 | 3.68093e-03 | | | |
| 1.49166e-02 | 4.06522e+00 | 3.66932e-03 | | | |
| 8.77733e-03 | 2.53519e+00 | 3.46220e-03 | | | |

- [1]
- [2] M. S. ALNÆS, J. BLECHTA, J. HAKE, A. JOHANSSON, B. KEHLET, A. LOGG, C. RICHARDSON, J. RING, M. E. ROGNES, AND G. N. WELLS, *The fenics project version 1.5*, Archive of Numerical Software, 3 (2015), <https://doi.org/10.11588/ans.2015.100.20553>.
- [3] V. ANAYA, Z. DE WIJN, D. MORA, AND R. RUIZ-BAIER, *Mixed displacement-rotation-pressure formulations for linear elasticity*, Comput. Methods Appl. Mech. Engrg., 344 (2019), pp. 71–94, <https://doi.org/10.1016/j.cma.2018.09.029>.
- [4] V. ANAYA, A. KHAN, D. MORA, AND R. RUIZ-BAIER, *Robust A Posteriori Error Analysis for Rotation-Based Formulations of the Elasticity/Poroelasticity Coupling*, SIAM J. Sci. Comput., 44 (2022), pp. B964–B995, <https://doi.org/10.1137/21M1427516>.
- [5] M. G. ARMENTANO AND V. MORENO, *A posteriori error estimates of stabilized low-order mixed finite elements for the Stokes eigenvalue problem*, J. Comput. Appl. Math., 269 (2014), pp. 132–149, <https://doi.org/10.1016/j.cam.2014.03.027>.
- [6] I. BABUŠKA AND J. OSBORN, *Handbook of numerical analysis. Vol. II*, (1991), pp. x+928. Finite element methods. Part 1.
- [7] T. P. BARRIOS, G. N. GATICA, M. GONZÁLEZ, AND N. HEUER, *A residual based a posteriori*

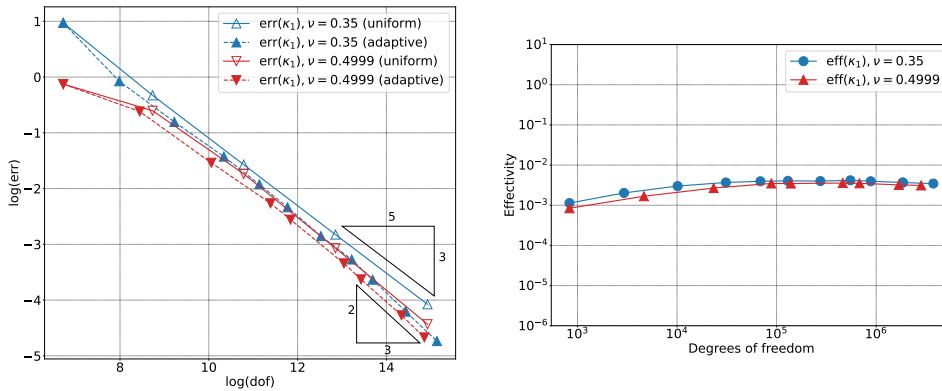


FIG. 14. *Test 4. Error and effectivity curves for $k = 1$, $\nu = 0.35$ and $\nu = 0.4999$.*

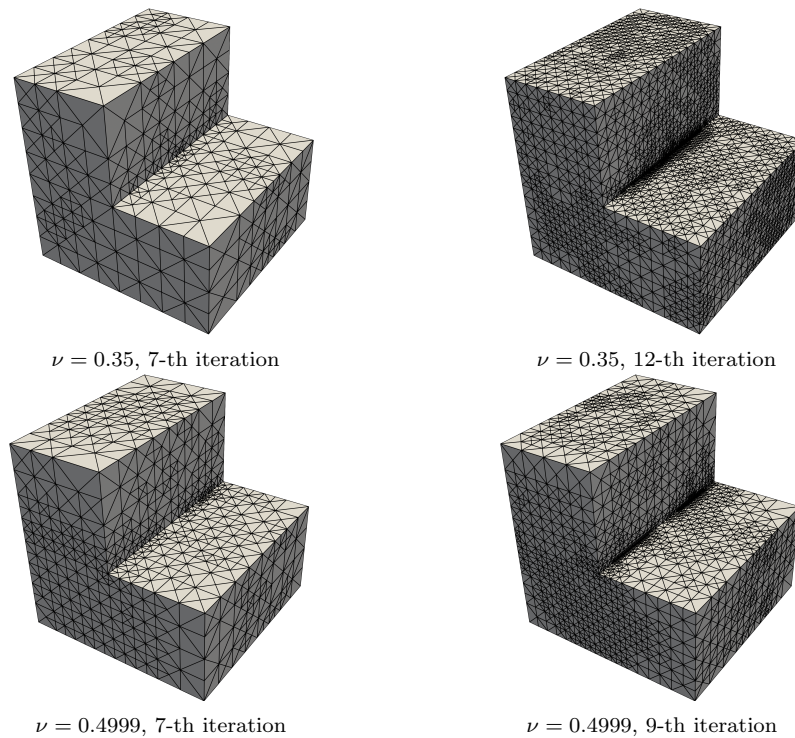


FIG. 15. *Test 4. Intermediate meshes in the adaptive refinement algorithm for $k = 1$, $\nu = 0.35$ and $\nu = 0.4999$.*

error estimator for an augmented mixed finite element method in linear elasticity, M2AN Math. Model. Numer. Anal., 40 (2006), pp. 843–869 (2007), <https://doi.org/10.1051/m2an:2006036>.

- [8] F. BERTRAND, D. BOFFI, AND R. MA, *An adaptive finite element scheme for the Hellinger-Reissner elasticity mixed eigenvalue problem*, Comput. Methods Appl. Math., 21 (2021), pp. 501–512, <https://doi.org/10.1515/cmam-2020-0034>.
- [9] D. BOFFI, F. BREZZI, AND L. GASTALDI, *On the convergence of eigenvalues for mixed formulations*, vol. 25, 1997, pp. 131–154 (1998). Dedicated to Ennio De Giorgi.
- [10] D. BOFFI, F. BREZZI, AND L. GASTALDI, *On the problem of spurious eigenvalues in the approximation of linear elliptic problems in mixed form*, Math. Comp., 69 (2000), pp. 121–140,

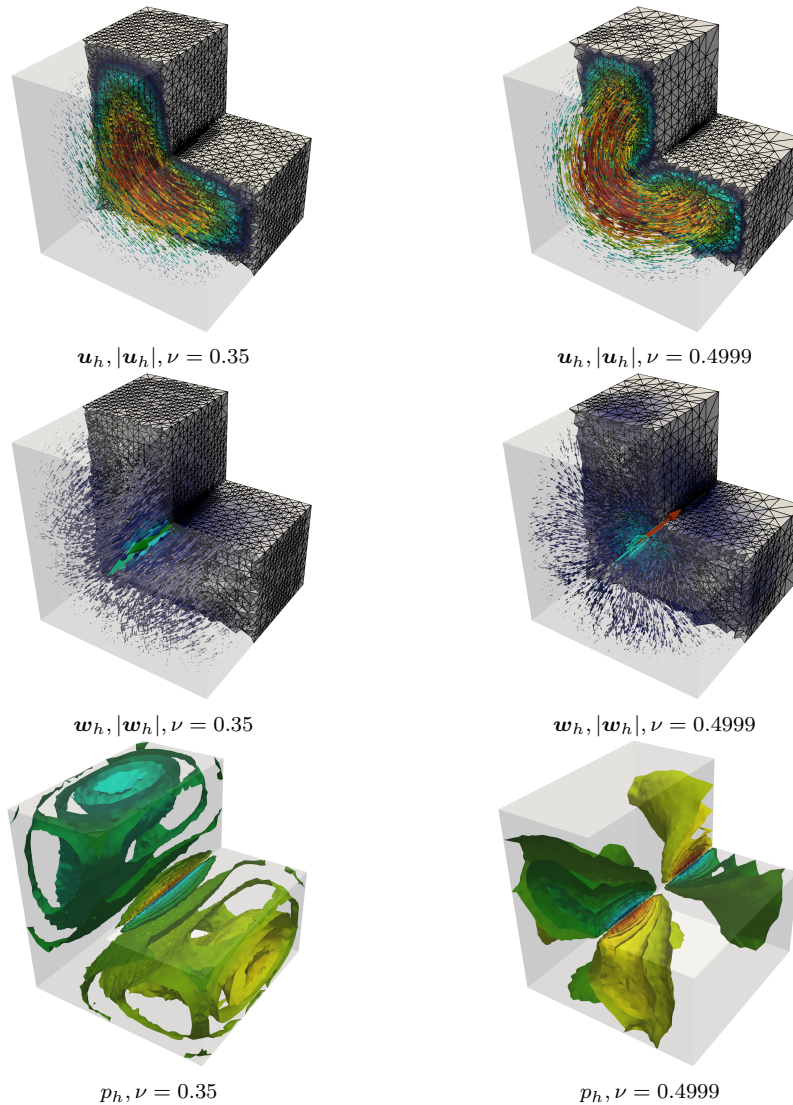


FIG. 16. Test 4. Lowest computed eigenmodes for $k = 1$ and different values of ν in the last adaptive iteration.

- <https://doi.org/10.1090/S0025-5718-99-01072-8>.
- [11] D. BOFFI, D. GALLISTL, F. GARDINI, AND L. GASTALDI, *Optimal convergence of adaptive FEM for eigenvalue clusters in mixed form*, Math. Comp., 86 (2017), pp. 2213–2237, <https://doi.org/10.1090/mcom/3212>.
- [12] C. CARSTENSEN AND J. GEDICKE, *Robust residual-based a posteriori Arnold-Winther mixed finite element analysis in elasticity*, Comput. Methods Appl. Mech. Engrg., 300 (2016), pp. 245–264, <https://doi.org/10.1016/j.cma.2015.10.001>.
- [13] P. G. CIARLET, *The finite element method for elliptic problems*, North-Holland Publishing Co., Amsterdam-New York-Oxford, 1978. Studies in Mathematics and its Applications, Vol. 4.
- [14] G. N. GATICA, L. F. GATICA, AND F. A. SEQUEIRA, *A $\mathbb{RT}_k - \mathbf{P}_k$ approximation for linear elasticity yielding a broken $H(\text{div})$ convergent postprocessed stress*, Appl. Math. Lett., 49 (2015), pp. 133–140, <https://doi.org/10.1016/j.aml.2015.05.009>.
- [15] G. N. GATICA, L. F. GATICA, AND F. A. SEQUEIRA, *A priori and a posteriori error analyses of a pseudostress-based mixed formulation for linear elasticity*, Comput. Math. Appl., 71

- (2016), pp. 585–614, <https://doi.org/10.1016/j.camwa.2015.12.009>.
- [16] C. GEUZAIN AND J.-F. REMACLE, *Gmsh: A 3-D finite element mesh generator with built-in pre-and post-processing facilities*, International journal for numerical methods in engineering, 79 (2009), pp. 1309–1331.
- [17] P. GRISVARD, *Problemes aux limites dans les polygones. mode d'emploi*, Bulletin de la Direction des Etudes et Recherches Series C Mathematiques, Informatique, 1 (1986), pp. 21–59.
- [18] T. HUGHES AND L. FRANCA, *A new finite element formulation for cfd: Vii. the stokes problem with various well-posed boundary conditions: Symmetric formulations that converge for all velocity/pressure spaces*, Comput. Methods Appl. Mech. Engrg, 65 (1987), pp. 85–96.
- [19] D. INZUNZA, F. LEPE, AND G. RIVERA, *Displacement-pseudostress formulation for the linear elasticity spectral problem: a priori analysis*, <https://arxiv.org/abs/2101.09828>, (2021), <https://arxiv.org/abs/2101.09828>, <https://arxiv.org/abs/2101.09828>.
- [20] T. KATO, *Perturbation theory for linear operators*, Die Grundlehren der mathematischen Wissenschaften, Band 132, Springer-Verlag New York, Inc., New York, 1966.
- [21] F. LEPE, S. MEDDAHI, D. MORA, AND R. RODRÍGUEZ, *Mixed discontinuous Galerkin approximation of the elasticity eigenproblem*, Numer. Math., 142 (2019), pp. 749–786, <https://doi.org/10.1007/s00211-019-01035-9>.
- [22] F. LEPE, D. MORA, AND R. RODRÍGUEZ, *Finite element analysis of a bending moment formulation for the vibration problem of a non-homogeneous Timoshenko beam*, J. Sci. Comput., 66 (2016), pp. 825–848, <https://doi.org/10.1007/s10915-015-0046-z>, <https://doi.org/10.1007/s10915-015-0046-z>.
- [23] A. MÁRQUEZ, S. MEDDAHI, AND T. TRAN, *Analyses of mixed continuous and discontinuous Galerkin methods for the time harmonic elasticity problem with reduced symmetry*, SIAM J. Sci. Comput., 37 (2015), pp. A1909–A1933, <https://doi.org/10.1137/14099022X>.
- [24] S. MEDDAHI, D. MORA, AND R. RODRÍGUEZ, *Finite element spectral analysis for the mixed formulation of the elasticity equations*, SIAM J. Numer. Anal., 51 (2013), pp. 1041–1063, <https://doi.org/10.1137/120863010>.
- [25] A. RÖSSLE, *Corner singularities and regularity of weak solutions for the two-dimensional lamé equations on domains with angular corners*, Journal of elasticity and the physical science of solids, 60 (2000), pp. 57–75.
- [26] L. R. SCOTT AND S. ZHANG, *Finite element interpolation of nonsmooth functions satisfying boundary conditions*, Math. Comp., 54 (1990), pp. 483–493, <https://doi.org/10.2307/2008497>, <https://doi.org/10.2307/2008497>.
- [27] R. VERFÜRTH, *A posteriori error estimation and adaptive mesh-refinement techniques*, in Proceedings of the Fifth International Congress on Computational and Applied Mathematics (Leuven, 1992), vol. 50, 1994, pp. 67–83, [https://doi.org/10.1016/0377-0427\(94\)90290-9](https://doi.org/10.1016/0377-0427(94)90290-9).
- [28] R. VERFÜRTH, *A posteriori error estimation techniques for finite element methods*, Numerical Mathematics and Scientific Computation, Oxford University Press, Oxford, 2013, <https://doi.org/10.1093/acprof:oso/9780199679423.001.0001>.